Crystallized Rate Regions for MIMO Transmission

Adrian Kliks, Pawel Sroka, Merouane Debbah

Hindawi Publishing Corporation
EURASIP Journal on Wireless Communications and Networking
Volume 2010, Article ID 919072, 17 pages
doi:10.1155/2010/919072

Research Article

Crystallized Rate Regions for MIMO Transmission

Adrian Kliks (EURASIP Member),[1] Pawel Sroka (EURASIP Member),[1] and Merouane Debbah[2]

[1] *Poznan University of Technology, Chair of Wireless Communications, Polanka 3, 60-965 Poznan, Poland*
[2] *SUPELEC, Alcatel-Lucent Chair on Flexible Radio, 3 rue Joliot-Curie, 91192 Gif-sur-Yvette, France*

Correspondence should be addressed to Pawel Sroka, psroka@et.put.poznan.pl

Received 1 February 2010; Revised 2 July 2010; Accepted 8 July 2010

Academic Editor: Osvaldo Simeone

When considering the multiuser SISO interference channel, the allowable rate region is not convex and the maximization of the aggregated rate of all the users by the means of transmission power control becomes inefficient. Hence, a concept of the crystallized rate regions has been proposed, where the time-sharing approach is considered to maximize the sumrate.In this paper, we extend the concept of crystallized rate regions from the simple SISO interference channel case to the MIMO/OFDM interference channel. As a first step, we extend the time-sharing convex hull from the SISO to the MIMO channel case. We provide a non-cooperative game-theoretical approach to study the achievable rate regions, and consider the Vickrey-Clarke-Groves (VCG) mechanism design with a novel cost function. Within this analysis, we also investigate the case of OFDM channels, which can be treated as the special case of MIMO channels when the channel transfer matrices are diagonal. In the second step, we adopt the concept of correlated equilibrium into the case of two-user MIMO/OFDM, and we introduce a regret-matching learning algorithm for the system to converge to the equilibrium state. Moreover, we formulate the linear programming problem to find the aggregated rate of all users and solve it using the Simplex method. Finally, numerical results are provided to confirm our theoretical claims and show the improvement provided by this approach.

1. Introduction

The future wireless systems are characterized by decreasing range of the transmitters as higher transmit frequencies are to be utilized. The decreasing cell sizes combined with the increasing number of users within a cell greatly increases the impact of interference on the overall system performance. Hence, mitigation of the interference between transmit-receive pairs is of great importance in order to improve the achievable data rates.

The Multiple Input Multiple Output (MIMO) technology has become an enabler for further increase in system throughput. Moreover, the utilization of spatial diversity thanks to MIMO technology opens new possibilities of interference mitigation [1–3].

Several concepts of interference mitigation have been proposed, such as the successive interference cancellation or the treatment of interference as additive noise, which are applicable to different scenarios [4–6]. When treating the interference as noise the, n-user achievable rates region has been found to be the convex hull of n hypersurfaces [7]. A novel strategy to represent this rate region in the n-dimensional space, by having only on/off power control has been proposed in [8]. A crystallized rate region is obtained by forming a convex hull by time-sharing between $2^n - 1$ corner points within the rate region [8].

Game-theoretic techniques based on the utility maximization problem have received significant interest [7–10]. The game-theoretical solutions attempt to find equilibria, where each player of the game adopts a strategy that they are unlikely to change. The best known and commonly used equilibrium is the Nash equilibrium [11]. However, the Nash equilibrium investigates only the individual payoff, and that may not be efficient from the system point of view. Better performance can be achieved using the correlated equilibrium [12], in which each user considers the others' behaviors to explore mutual benefits. In order to find the correlated equilibrium, one can formulate the linear programming

problem and solve it using one of the known techniques, such as the Simplex algorithm [13]. However, in case of MIMO systems, the number of available game strategies is high, and the linear programming solution becomes very complex. Thus, a distributed solution can be applied, such as the regret-matching learning algorithm proposed in [8], to achieve the correlated equilibrium at lower computational cost. Moreover, the overall system performance may be further improved by an efficient mechanism design, which defines the game rules [14].

In this paper, the rate region for the MIMO interference channel is examined based on the approach presented in [8, 15]. Specific MIMO techniques have been taken into account such as transmit selection diversity, spatial water-filling, SVD-MIMO, or codebook-based beamforming [16–19]. Moreover, an application of the correlated equilibrium concept to the rate region problem in the considered scenario is presented. Furthermore, a new Vickey-Clarke-Groves (VCG) auction utility [11] formulation and the modified regret-matching learning algorithm are proposed to demonstrate the application of the considered concept for the 2-user MIMO channel.

The reminder of this paper is structured as follows. Section 2 presents the concept of crystallized rates region for MIMO transmission. Section 3 describes the application of correlated equilibrium concept in the rate region formulation and presents the linear programming solution for the sum-rate maximization problem. Section 4 outlines the mechanism design for application of the proposed concept in 2-user interference MIMO channel, comprising the VCG auction utility formulation and the modified regret-matching learning algorithm. Moreover, specific cases of different MIMO precoding techniques, including the ones considered for future 4G systems such as the Long Term Evolution-Advanced (LTE-A) [20, 21], and Orthogonal Frequency Division Multiplexing (OFDM) transmission are presented as examples of application of the derived model. Finally, Section 5 summarizes the simulation results obtained for the considered specific cases, and Section 6 draws the conclusions.

2. Crystallized Rate Regions for MIMO/OFDM Transmission

In this section, we present the generalization of the concept of crystallized rate regions in the context of the OFDM/MIMO transmissions. We start with defining the channel model under study and follow by the analysis of the achievable rate regions for the interference MIMO channel, when interference is treated as Gaussian noise. Finally, the generalized definition of the rate regions for the MIMO/OFDM transmission will be presented.

2.1. System Model for 2-User Interference MIMO Channel. The multicell uplink interference MIMO channel is considered in this paper. Without loss of generality and for the sake of clarity, the channel model consists in the 2-user 2-cell scenario, in which each user (denoted as the Mobile Terminal (MT)) communicates with his own Base Station (BS) causing interference to the neighboring cell (see Figure 1(a)). Each MT is equipped with N_t (transmit) antennas, and each BS has N_r (receive) antennas. Moreover, user i can transmit data with maximum total power $P_{i,\,\max}$. Perfect channel knowledge in all MTs is assumed. In order to ease the analysis, we limit our derivation to the 2×2 MIMO case (see Figure 1(b)), where both the transmitter and the receiver use only two antennas.

User i transmits the signal vector $X_i \in \mathbf{C}^2$ through the multipath channel $\mathbf{H} \in \mathbf{C}^{4\times 4}$, where

$$\mathbf{H} = \begin{pmatrix} \mathbf{H}_{11} & \mathbf{H}_{12} \\ \mathbf{H}_{21} & \mathbf{H}_{22} \end{pmatrix}, \qquad \mathbf{H}_{i,\,j} \in \mathbb{C}^{2\times 2}. \tag{1}$$

The channel matrix $\mathbf{H}_{i,\,j} = \{h_{k,\,l}^{(i,\,j)} \in \mathbb{C},\ 1 \le k, l \le 2\}$ consists of the actual values of channel coefficients $h_{k,\,l}^{(i,\,j)}$, which define the channel between transmit antenna k at the ith MT and the receive antenna l at the jth BS. In the considered 2-user 2×2 MIMO case, only four channel matrices are defined, that is, $\mathbf{H}_{11}$, $\mathbf{H}_{22}$ (which describe channel between the first MT and first BS or second MT and second BS, resp.), $\mathbf{H}_{12}$, and $\mathbf{H}_{21}$ (which describe the interference channel between first MT and second BS and between second MT and first BS, resp.). Additive White Gaussian Noise (AWGN) of zero mean and variance σ^2 is added to the received signal. Receiver i observes the useful signal, denoted as Y_i, coming from the ith user. Moreover, in the interference scenario, receiver i (BS_i) receives also interfering signals from other users located at the neighboring cell $Y_j,\ j \ne i$. Interested readers can find solid contribution on the interference channel capacity in the rich literature, for example, [1, 2, 22, 23]. When interference is treated as noise, the achievable rates for 2-user interference MIMO channel are defined as follows [22]:

$$\begin{aligned} R_1(\mathbf{Q}_1,\ \mathbf{Q}_2) &= \log_2\Big(\det\Big(\mathbf{I} + \mathbf{H}_{11}\mathbf{Q}_1\mathbf{H}_{11}^* \\ &\qquad \cdot \left(\sigma^2\mathbf{I} + \mathbf{H}_{21}\mathbf{Q}_2\mathbf{H}_{21}^*\right)^{-1}\Big)\Big), \\ R_2(\mathbf{Q}_1,\ \mathbf{Q}_2) &= \log_2\Big(\det\Big(\mathbf{I} + \mathbf{H}_{22}\mathbf{Q}_2\mathbf{H}_{22}^* \\ &\qquad \cdot \left(\sigma^2\mathbf{I} + \mathbf{H}_{12}\mathbf{Q}_1\mathbf{H}_{12}^*\right)^{-1}\Big)\Big), \end{aligned} \tag{2}$$

where R_1 and R_2 denote the rate of the first and second user, respectively, $(\mathbf{A}^*)$ denotes transpose conjugate of matrix $\mathbf{A}$, $\det(\mathbf{A})$ is the determinant of matrix $\mathbf{A}$, and $\mathbf{Q}_i$ is the ith user data covariance matrix, that is, $E\{X_iX_i^*\} = \mathbf{Q_i}$ and $\mathrm{tr}(\mathbf{Q}_1) \le P_{1,\max}$, $\mathrm{tr}(\mathbf{Q}_2) \le P_{2,\max}$. We define the rate region as $\Re = \bigcup\{(R_1(\mathbf{Q}_1,\ \mathbf{Q}_2),\ R_2(\mathbf{Q}_1,\ \mathbf{Q}_2))\}$.

One can state that the formulas presented above allow us to calculate the rates that can be achieved by the users in the MIMO interference channel scenario in a particular case when no specific MIMO transmission technique is applied. Such approach can be interpreted as a so-called Transmit Selection Diversity (TSD) MIMO technique [16], where the BS can decide between one of the following strategies: to put all of the transmit power to one antenna (N_t strategies, where N_t is the number of antennas), to be silent (one strategy), or to equalize the power among all antennas (one strategy).

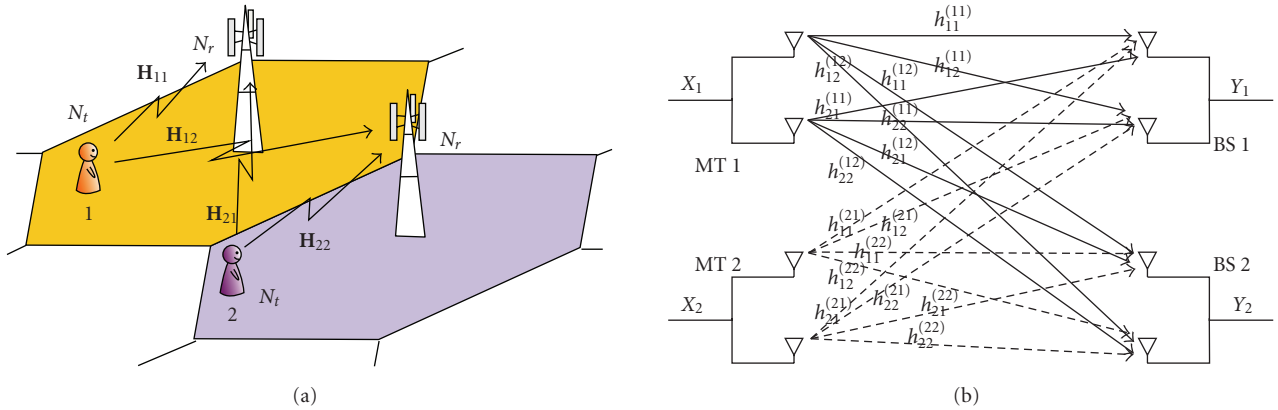

FIGURE 1: MIMO interference channel: general 2-cell 2-user model (a) and the details representation of the considered 2×2 case (b).

When the channel is known at the transmitter, the channel capacity can be optimized by means of some well-known MIMO transmission techniques. Precisely, one can decide for example to linearize (diagonalize) the channel by the means of Eigenvalue Decomposition (EvD) or Singular Value Decomposition (SVD) [16, 17, 24]. Such approach will be denoted hereafter as SVD-MIMO.v Moreover, in order to avoid or minimize the interference between the neighboring users within one cell, BS can precode the transmit signal. In such a case, the sets of properly designed transmit and receive beamformers are used at the transmitter and receiver side, respectively. The precoders can be either calculated continuously based on the actual channel state information from all users or can be defined in advance (predefined) and stored in a form of a codebook, from which the optimal set of beamformers is selected for each user based on its channel condition. The later approach is proposed in the Long Term Evolution (LTE) standard where for the 2×2 MIMO case a specific codebook is proposed [20]. Similar assumption is made for the so called Per-User Unitary Rate Control (PU^{2}RC) MIMO systems, where the set of N beamformers is calculated [18, 21]. Since the process of finding the set of transmit and receive beamformers is usually time and energy consuming and require accurate Channel State Information (CSI), the optimal approaches (where the precoders are calculated based on the actual channel state) are replaced by the above-mentioned list of predefined beamformers stored in a form of a codebook. Since the number of precoders is limited, the performance of such approach could be worse than the optimal one, particularly in the interference channel scenario. Based on this observation, new techniques of generation of the set of N beamformers have been proposed. One of them is called random-beamforming [19, 25], since the set of precoders is obtained in a random manner. At every specified time instant, a new set of beamformers is randomly generated, from which the subset of precoders that optimize some predefined criteria is selected. Simulation results given in [19, 25] and Section 5.1 show that assuming such approach, one can achieve the global extremum in particular when the codebook size is large. When the set of randomly generated beamformers is used, the set of receive beamformers has to be calculated at the receiver. Various criteria can be used, just to mention the most popular and academic ones: Zero-Forcing (ZF), MinimumMean Squared Error (MMSE), or Maximum-Likelihood (ML) [16, 17]. In our simulation, we consider the combination of these methods, that is, ZF-MIMO, MMSE-MIMO, and ML-MIMO, with three different codebook generation methods—one of the size N, that is, generated randomly (denoted hereafter as RAN-N), one defined as proposed for LTE and one specified for PU^{2}RC-MIMO. In other words, the abbreviation ZF-MIMO-LTE describes the situation when the transmitter uses the LTE codebook and the set of receive beamformers is calculated using the ZF criterion.

However, let us stress that (2) has to be modified when one of the precoding techniques (including SVD method, which is a particular case of precoding) is applied. Thus, the general equations for the achievable rate computation are defined as follows:

$$\begin{aligned} R_1(\mathbf{Q}_1, \mathbf{Q}_2) &= \log_2\Big(\det\Big(\mathbf{I} + \mathbf{u}_1^*\mathbf{H}_{11}\mathbf{v}_1\mathbf{Q}_1\mathbf{v}_1^*\mathbf{H}_{11}^*\mathbf{u}_1 \\ &\qquad \cdot \left(\sigma^2\mathbf{u}_1^*\mathbf{u}_1 + \mathbf{u}_1^*\mathbf{H}_{21}\mathbf{u}_2\mathbf{Q}_2\mathbf{u}_2\mathbf{H}_{21}^*\mathbf{u}_1\right)^{-1}\Big)\Big), \\ R_2(\mathbf{Q}_1, \mathbf{Q}_2) &= \log_2\Big(\det\Big(\mathbf{I} + \mathbf{u}_2^*\mathbf{H}_{22}\mathbf{v}_2\mathbf{Q}_2\mathbf{v}_2^*\mathbf{H}_{22}^*\mathbf{u}_2 \\ &\qquad \cdot \left(\sigma^2\mathbf{u}_2^*\mathbf{u}_2 + \mathbf{u}_2^*\mathbf{H}_{12}\mathbf{u}_1\mathbf{Q}_1\mathbf{u}_1\mathbf{H}_{12}^*\mathbf{u}_2\right)^{-1}\Big)\Big), \end{aligned} \tag{3}$$

where $\mathbf{u}_i$ and $\mathbf{v}_i$ denote the set of receive and transmit beamformers, respectively, obtained for the ith user. In a case of SVD-MIMO, the above-mentioned vectors are obtained by the means of singular value decomposition of the channel transfer matrix whereas for the other precoded MIMO systems, the set of receive coefficients is calculated as follows [23]:

(i) for zero-forcing receiver

$$\mathbf{v}_i = \left(\left(\mathbf{H}_{ii}^*\mathbf{H}_{ii}\right)^{-1} \cdot \mathbf{H}_{ii}^*\right)^*, \tag{4}$$

(ii) for MMSE receiver

$$\mathbf{v}_i = \left(\left(\mathbf{H}_{ii}^{*}\mathbf{H}_{ii} + \sum_{\substack{j \\ j \neq i}} \frac{P_j}{P_i} \mathbf{H}_{ji}^{*}\mathbf{H}_{ji} + \sigma^2 \mathbf{I} \right)^{-1} \cdot \mathbf{H}_{ii}^{*} \right)^{*}, \quad (5)$$

(iii) for the ML receiver the elements of receive beamformers are equal to 1 (in other words, no receive beamforming is used).

The last Hermitian conjugate in (4) and in (5) is due to the assumed definition of the achievable user rates in (3).

For comparison purposes, the spatial waterfilling technique will be considered [26], where the transmit power is distributed among the antennas based on the waterfilling algorithm. The spatial waterfilling approach will be denoted hereafter as SWF-MIMO.

2.2. Achievable Rate Regions in a Case of TSD-MIMO Interference Channel. In [8], the achievable rate regions in the 2-user SISO scenario have been studied, where the authors have treated the interference as Gaussian noise. It has been stated that the rate region for the general n-user channel is found to be the convex hull of the union of n hyper-surfaces [7], which means that the rate regions entirely encloses a straight line that connects any two points which lie within the rate region bounds. In the 2-user case, the rate regions can be easily represented as the surface limited by the horizontal and vertical axes and the boundaries of the 2-dimensional hypersurface (straight lines). Let us stress that the same conclusions can be drawn for the MIMO case. We will then discuss various achievable rate regions for the interference MIMO channel. We will analyze the properties of the rate regions introduced below in three cases: when the results are averaged over 2000 channel realizations (Case A) and for specific channel realizations (Cases B and C).

2.2.1. Rate Region for TSD-MIMO Interference Channel Case A. The rate region for the general interference TSD-MIMO channel is depicted in Figure 2. The results have been obtained based on the assumption that both users transmit with the same uniform power $P_{i,\max} = 1$ and the results have been averaged over 2000 channel realizations, for $h_{k,l}^{(i,j)} \sim \mathcal{CN}(0, 1, 0)$. One can define three characteristic points on the border of the rate region, that is, points A, B, and C. Specifically, point A describes the situation, where the first user transmits with the maximum power, and $\mathbf{Q}_1$ is chosen such that $\mathbf{Q}_1 = \arg\max_{\tilde{\mathbf{Q}}_1} R_1(\tilde{\mathbf{Q}}_1, \mathbf{Q}_2 = \mathbf{0})$. Point C can be defined in the same way as point A, but with reference to the second user. Point B corresponds to the situation, where both users transmit with the maximum power and the distribution of the power among the antennas is optimal in the sum-rate sense, that is, $(\mathbf{Q}_1, \mathbf{Q}_2) = \arg\max_{\tilde{\mathbf{Q}}_1, \tilde{\mathbf{Q}}_2} (R_1(\tilde{\mathbf{Q}}_1, \tilde{\mathbf{Q}}_2) + R_2(\tilde{\mathbf{Q}}_1, \tilde{\mathbf{Q}}_2))$. The first frontier line $\Phi_{\mathrm{AB}} = \Phi(\mathbf{Q}_{1,p}, :)$, $p = P_{1,\max}$, (where $\mathbf{Q}_{i,p}$ denotes the covariance for which $\mathrm{tr}(\mathbf{Q}_i) = p$) is obtained when holding the total transmit power for the first user fixed and varying the total transmit power for the second user from zero to $P_{2,\max}$. Similarly, the second frontier line $\Phi_{\mathrm{BC}} = \Phi(:, \mathbf{Q}_{2,p})$, $p = P_{2,\max}$, is characterized by holding the total transmit power of the second user fixed to $P_{2,\max}$ and decreasing the total transmit power by the first user from $P_{1,\max}$ to zero. One can observe that the achievable rate region for the two user 2×2 MIMO case is not convex, thus the time-sharing (see Section 2.5) approach seems to be the right way for system capacity improvement. The potential time-sharing lines are also presented in Figure 2.

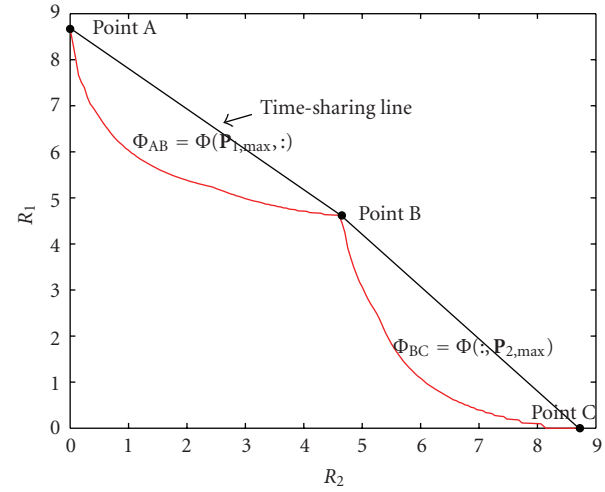

FIGURE 2: Achievable rate region for the MIMO interference channel—averaged over 2000 channel realizations.

2.2.2. Rate Region for TSD-MIMO Interference Channel Case B. Quite different conclusions can be drawn for a specific channel realization (i.e., the obtained rate regions are not averaged over many channel realizations), where the second user receives strong interference (see Figure 3). In such a case, new characteristic points can be indicated on the frontier lines of the achieved rate region. While the points A and C can be defined in the same way as in the previous case (i.e., when the results were averaged), two new points D and E appeared. All of the characteristic points define a combination of four possible situations. These are: (a) user i balances all the power on the first antenna (b) user i balances all the power on the second antenna (c) user i divides the transmit power in an optimal way among both antennas (d) user i does not transmit. When both users chose one of the four predefined strategies, one of the characteristic points (in our case points A, C, D, and E) on the frontier line of the rate regions can be reached. In Figure 3 the potential time-sharing lines are also plotted.

2.2.3. Rate Region for TSD-MIMO Interference Channel Case C. In Figure 4, the results obtained for another fixed channel realization are presented mainly a case is considered, where the first user transmits data with twice the maximum power (i.e., $P_{1,\max} = 2 \cdot P_{2,\max}$) of user 2. One can observe that user 1 achieves significantly higher rates compared to user 2. For this situation, similar conclusions can be drawn as for

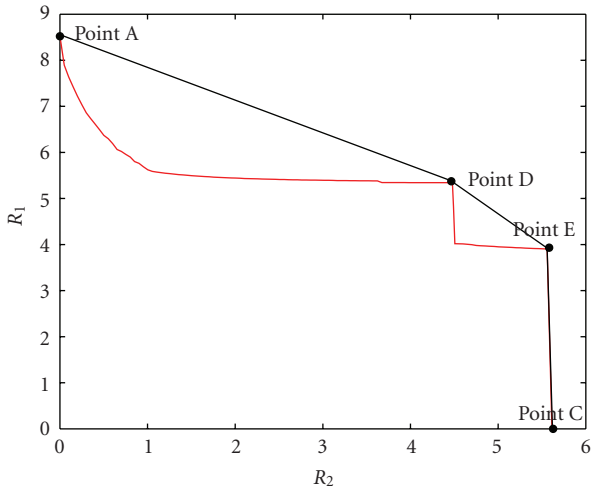

Figure 3: Achievable rate region for the MIMO interference channel—one particular channel realization (user two observes strong interference).

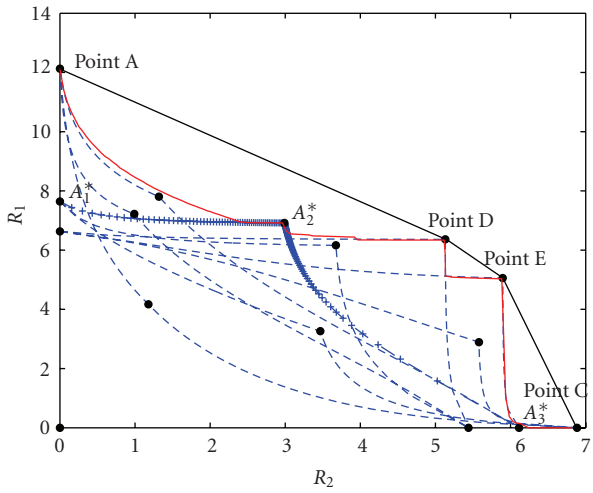

Figure 4: Achievable rate region for the MIMO interference channel—the transmit power of the first user is twice higher than the transmit power of the second user.

the situation depicted in Figure 3, that is, new characteristic points have occurred.

Let us put the attention on the additional dashed curves which are enclosed inside the rate region and usually start and finish in one of the characteristic points (depicted as small black-filled circles). These curves show the rate evolution achieved by both users when the users decide to choose one of the four predefined strategies. Let us define them explicitly: user i does not transmit any data (strategy $\alpha_i^{(0)}$), puts all the transmit power to the antenna number 1 (strategy $\alpha_i^{(1)}$) or 2 (strategy $\alpha_i^{(2)}$), or distribute the total power equally between both antennas (strategy $\alpha_i^{(3)}$). For example, the line with the plus marks denotes the following user behavior: starting from point A_1^*, when the first user transmits all the power on the first antenna and the second

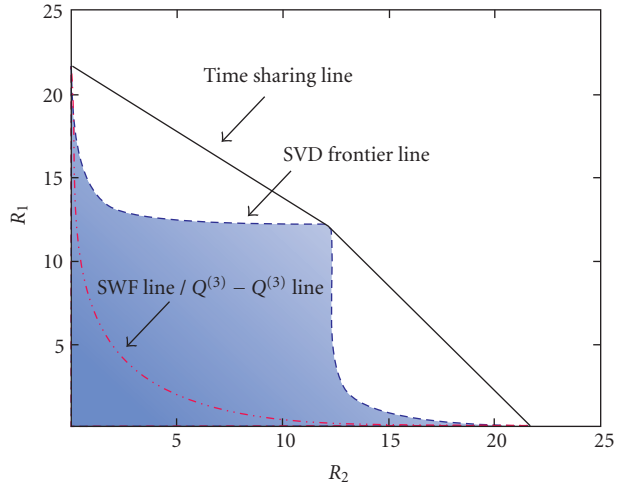

Figure 5: Achievable rate region for the precoded MIMO interference channel.

user is silent, the second user increases the transmit power on the second antenna from zero to $P_{2,\max}$ achieving point A_2^*; user 2 transmits with fixed power on the second antenna, and the first user reduces the power from the $P_{1,\max}$ to zero reaching point A_3^*. In other words, this line corresponds to the situation when user 1 chooses strategy $\alpha^{(1)}$, and the user 2 selects strategy $\alpha^{(2)}$. The other lines below the frontiers show what rate will be achieved by both users when they decide to play one of the predefined strategies all the time. Let us notice that choosing the strategy $\alpha^{(0)}$ by one of the user results in moving over the vertical or horizontal border of the achievable rate region. However, such a case will not be discussed in this paper. It is worth mentioning that the frontier lines define the boundaries of the rate region that corresponds to choosing the best strategy in every particular situation by both users. In other words, the frontier line is more or less similar to the rate achieved by both users when every time both of them select the best strategy for the actual value of transmit power, what can be approximated as switching between the dashed lines in order to maximize the instantaneous throughput?

2.3. Achievable Rate Regions for the Precoded MIMO Systems. Similar analysis can be applied for the SVD-MIMO case. In such a situation, the BS can also select one of the four strategies defined in the previous subsection however, the precoder is computed in an (sub) optimal way by the means of SVD based on the information on the channel transfer function. The channel transfer functions $\mathbf{H}_{ij}$ that define the channel between user in the ith cell and the jth BS in a jth cell are assumed to be unknown by the neighboring BSs. An exemplary plot of the achievable rate region for 2000 channel realizations is presented in Figure 5. One can observe that the obtained rate region is concave, thus the time-sharing approach seems to provide better results. As in a TSD-MIMO case, the obtained results are characterized by a higher number of corner points (degrees of freedom) when compared to the Single-Input/Single-Output (SISO)

transmission. The transmitter can select one of the corner points in order to optimize some predefined criteria (like minimization of interference between users). The spatial waterfilling line is also shown in this figure which matches the $Q^{(3)} - Q^{(3)}$ line (i.e., the line when both users choose the third strategy with equally distributed power among transmit antennas every time and control the transmit power to maximize the capacity). Let us stress the difference between the SWF-line and the SVD frontier line. The former is obtained as follows: user 1 transmit with the maximum allowed power $P_{\max}$ using SWF technique and at the same time user 2 increases its power from 0 to $P_{\max}$. Next, the situation is reversed—the second user transmits with maximum allowed power and user 1 reduces the transmit power from $P_{\max}$ to 0. In other words, the covariance matrix $\mathbf{Q}_x$ is simply the identity matrix multiplied by the actual transmit power. Contrary to this case, the SVD frontier line represents the maximum possible rates that can be achieved by both users for every possible realization of the covariance matrix $\mathbf{Q}_x$, whose trace is less or equal to the maximum transmit power, and when precoding based on SVD of the channel transfer function has been applied. The frontier line defines the maximum theoretic rates that can be achieved by both users. One can observe that although both lines start and end at the same points of the achievable rate region, the influence of interference is significantly higher in the SWF approach.

2.4. Achievable Rate Regions for the OFDM Systems. The methodology proposed in the previous sections can be also applied in a case of OFDM transmission. In such a case, the interferences will be observed only in a situation, when the neighboring users transmit data on the same subcarrier. Two achievable rate regions for OFDM transmission are presented below that is, in Figure 6, the rate region averaged over 2000 different channel realizations is shown, and in Figure 7, the rate region achieved for one arbitrarily selected channel realization are presented (in particular, the channel between the first user and its BS was worse than the second user-channel attenuation was higher, and the maximum transmit power of the second user was twice higher than for the first one). In both figures, the time-sharing lines are plotted. Moreover, the curves that show the rate region boundaries when the users play one specific strategy all the time are shown (represented as the dashed lines in the figure).

The obtained results are similar to those achieved for the MIMO case. However, some significant differences can be found, like the difference in the achievable rates in general—the maximum achievable rates are lower in a OFDM case comparing to the MIMO scenario.

2.5. Crystallized Rate Regions and Time-Sharing Coefficients for the MIMO Transmission. The idea of the crystallized rate regions has been introduced in [8] and can be understood as an approximation of the achievable rate regions by the convex time-sharing hull, where the potential curves between characteristic points (e.g., A, B, and C in Figure 2) are replaced by the straight lines connecting these points.

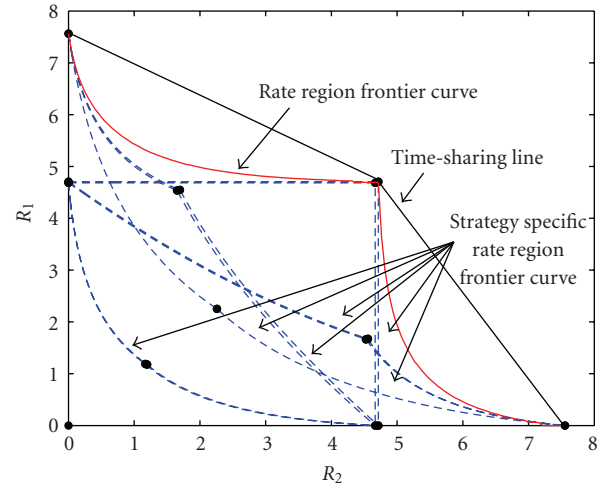

Figure 6: Achievable rate region for the OFDM interference channel—results averaged over 2000 channel realizations.

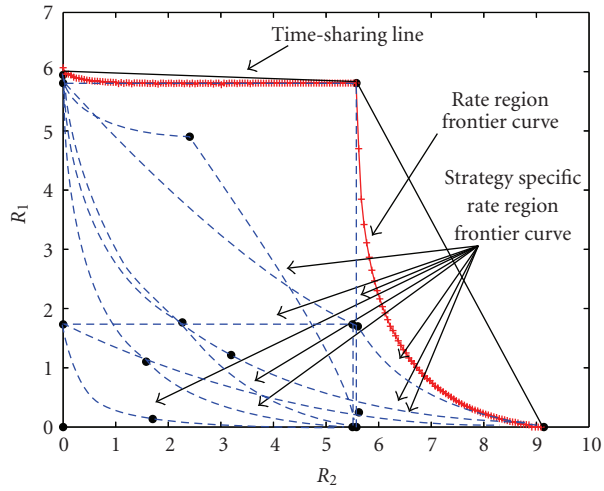

Figure 7: Achievable rate region for the OFDM interference channel—one particular channel realization, maximum transmit power of the first user is two times higher than the maximum transmit power of the second user.

One can observe from the results shown in Figure 4 that for the MIMO case, the crystallized rate region for the 2-user scenario has much more characteristic points (i.e., the points where both users transmit with the maximum power for selected strategy) than in the SISO case (see [8] for comparison). In order to create the convex hull, only such points can be selected, which lie on the frontier line. Moreover, the selection of all characteristic points that lie on border line could be nonoptimal, thus only a subset of these points should be chosen for the time-sharing approach (compare Figures 3 and 4).

Let us denote each point in the rate region as $\Phi(\mathbf{Q}_{1,\,p_1}, \mathbf{Q}_{2,\,p_2})$, that is, $\mathrm{tr}(\mathbf{Q}_{1,\,p_1}) = p_1$, $0 \le p_1 \le P_{1,\max}$ and $\mathrm{tr}(\mathbf{Q}_{2,\,p_2}) = p_2$, $0 \le p_2 \le P_{2,\max}$. Point A in Figure 2 can be defined as $\Phi(\mathbf{P}_{1,\max}, 0)$; that is, user one transmits with the maximum total power and the second user is silent; point C, as $\Phi(0, \mathbf{P}_{2,\max})$; that is, the first user does not transmit

any data and the second user transmits with the maximum total power; point B is defined as $\Phi(\mathbf{P}_{1,\max},\ \mathbf{P}_{2,\max})$; that is, both users transmit with the maximum total power. One can observe that these points are corner (characteristic) points of the achievable rate region. In the 2-user 2×2 TSD-MIMO channel, there exist 15 points, which refer to any particular combination of the possible strategies. In general, for the n-user $N_t \times N_r$ MIMO case, there exist $(N_t + 2)^n - 1$ points; that is, the ith user can put all power to one antenna (N_t possibilities), divide the power equally among the antennas (one possibility), or be silent (one possibility). We do not take into account the case when all users are silent. In a SISO case, $N_t = 1$ and the number of strategies is limited to two (i.e., the division of the power equally among all antennas denotes that all the power is transmitted through the antenna).

Following the approach proposed in [8], we state that instead of power control problem in finding the metrics $\mathbf{P}_i$, the problem becomes finding the appropriate time-sharing coefficients of the $(N_t + 2)^n - 1$ corner points. For the 2-user 2×2 TSD-MIMO case, we will obtain 15 points, that is, $\boldsymbol{\Theta} = [\theta_{k,l}]$ for $0 \le k, l \le 3$, which fulfill $\sum_{k,l} \theta_{k,l} = 1$. In our case, the time-sharing coefficients relate to the specific corner points; that is, the coefficient $\theta_{k,l}$ defines the point, where user 1 choose the strategy $\alpha_1^{(k)}$ and user 2 selects the strategy $\alpha_2^{(l)}$. Consequently, (2) can be rewritten as in (6), where $\mathbf{Q}_i^{(k)}$ denotes the ith user covariance matrix while choosing the strategy $\alpha_i^{(k)}$. Let us stress that any solution point on the crystallized rate border line (frontier) will lie somewhere on the straight lines connecting any of the neighboring characteristic points.

$$\begin{aligned} R_1(\boldsymbol{\Theta}) &= \sum_{k,l} \theta_{k,l} \cdot \log_2\Big(\det\Big(\mathbf{I} + \mathbf{H}_{11}\mathbf{Q}_1^{(k)}\mathbf{H}_{11}^* \\ &\qquad \cdot \Big(\sigma^2\mathbf{I} + \mathbf{H}_{21}\mathbf{Q}_2^{(l)}\mathbf{H}_{21}^*\Big)^{-1}\Big)\Big), \\ R_2(\boldsymbol{\Theta}) &= \sum_{k,l} \theta_{k,l} \cdot \log_2\Big(\det\Big(\mathbf{I} + \mathbf{H}_{22}\mathbf{Q}_2^{(l)}\mathbf{H}_{22}^* \\ &\qquad \cdot \Big(\sigma^2\mathbf{I} + \mathbf{H}_{12}\mathbf{Q}_1^{(k)}\mathbf{H}_{12}^*\Big)^{-1}\Big)\Big). \end{aligned} \tag{6}$$

Similar conclusions can be drawn for the precoded MIMO systems, where (6), that defines the achievable rate in a time-sharing approach, has to be rewritten in order to include the transmit and receive beamformers set (see (7))

$$\begin{aligned} &R_1(\boldsymbol{\Theta}) \\ &= \sum_{k,l} \theta_{k,l} \cdot \log_2\Big(\det\Big(\mathbf{I} + \mathbf{u}_1^*\mathbf{H}_{11}\mathbf{v}_1\mathbf{Q}_1^{(k)}\mathbf{v}_1^*\mathbf{H}_{11}^*\mathbf{u}_1 \\ &\qquad \cdot \Big(\sigma^2\mathbf{u}_1^*\mathbf{u}_1 + \mathbf{u}_1^*\mathbf{H}_{21}\mathbf{v}_2\mathbf{Q}_2^{(l)}\mathbf{v}_2^*\mathbf{H}_{21}^*\mathbf{u}_1\Big)^{-1}\Big)\Big) \\ &R_2(\boldsymbol{\Theta}) \\ &= \sum_{k,l} \theta_{k,l} \cdot \log_2\Big(\det\Big(\mathbf{I} + \mathbf{u}_2^*\mathbf{H}_{22}\mathbf{v}_2\mathbf{Q}_2^{(l)}\mathbf{v}_2^*\mathbf{H}_{22}^*\mathbf{u}_2 \\ &\qquad \cdot \Big(\sigma^2\mathbf{u}_2^*\mathbf{u}_2 + \mathbf{u}_2^*\mathbf{H}_{12}\mathbf{v}_1\mathbf{Q}_1^{(k)}\mathbf{v}_1^*\mathbf{H}_{12}^*\mathbf{u}_2\Big)^{-1}\Big)\Big). \end{aligned} \tag{7}$$

3. Correlated Equilibrium for Crystallized Interference MIMO Channel

In general, each user plays one of $N_s = N_c + 2$ strategies $\alpha^{(k)}$, $1 \le k \le N_c$, where N_c is the number of antennas in case of TSD-MIMO and SVD-MIMO ($N_c = N_t$) whereas for ZF/MMSE/ML-MIMO N_c denotes the codebook size ($N_c = N$). As a result of playing one of the strategies, the ith user will receive payoff, denoted hereafter $U_i(\alpha_i^{(k)})$. The aim of each user is to maximize its payoff with or without cooperation with the other users. Such a game leads to the well-known Nash equilibrium strategy α_i^* [27], such that

$$U_i(\alpha_i^*,\ \boldsymbol{\alpha}_{-i}) \ge U_i(\alpha_i,\ \boldsymbol{\alpha}_{-i}), \qquad \forall i \in S, \tag{8}$$

where α_i represents the possible strategy of the ith user whereas $\boldsymbol{\alpha}_{-i}$ defines the set of strategies chosen by the other users, that is, $\boldsymbol{\alpha}_{-i} = \{\alpha_j\}$, $j \ne i$, and S is the users set of the cardinality n. The idea behind the Nash equilibrium is to find the point of the achievable rate region (which is related to the selection of one of the available strategies), from which any user cannot increase its utility (increase the total payoff) without reducing other users' payoffs.

Moreover, in this context, the correlated equilibrium used in [8] instead of the Nash equilibrium is defined as α_i^* such that

$$\begin{aligned} \sum_{\boldsymbol{\alpha}_{-i} \in \Omega_{-i}} & p(\alpha_i^*,\ \boldsymbol{\alpha}_{-i})\left[U_i(\alpha_i^*,\ \boldsymbol{\alpha}_{-i}) - \mathrm{U}_i(\alpha_i,\ \boldsymbol{\alpha}_{-i})\right] \\ &\ge 0, \qquad \forall \alpha_i, \alpha_i^* \in \Omega_i,\ \forall i \in S, \end{aligned} \tag{9}$$

where $p(\alpha_i^*,\ \boldsymbol{\alpha}_{-i})$ is the probability of playing strategy α_i^* in a case when other users select their own strategies α_j, $j \ne i$. Ω_i and Ω_{-i} denote the strategy space of user i and all the users other than i, respectively. The probability distribution p is a joint point mass function of the different combinations of users strategies. As in [8], the inequality in correlated equilibrium definition means that when the recommendation to user i is to choose action α_i^*, then choosing any other action instead of α_i^* cannot result in higher expected payoff for this user. Note that the cardinality of the Ω_{-i} is $(N_c + 2)^{(n-1)}$.

Let us stress out that the time-sharing coefficients $\theta_{k,l}$ are the $(N_c + 2)^{(n-1)}$ point masses that we want to compute. In such a case, the one-to-one mapping function between any time-sharing coefficient $\theta_{k,l}$ and the corresponding point mass function $p(\alpha_i^{(k)}, \alpha_j^{(l)})$ of the point $\Phi(\alpha_i^{(k)}, \alpha_j^{(l)})$ can be defined as follows:

$$\theta_{k,l} = p\left(\alpha_i^{(k)},\ \alpha_j^{(l)}\right), \tag{10}$$

where $p(\alpha_i^{(k)},\ \alpha_j^{(l)})$ is the probability of user i playing the kth strategy and user j playing the lth strategy.

3.1. The Linear Programming (LP) Solution. Let us formulate the LP problem of finding the optimal time-sharing coefficients $\theta_{k,l}$. Following [28, 29] and for the sake of simplicity, we limit the problem to the sum-rate maximization (the weighted sum) as presented below:

$$\begin{aligned}
\arg\max_{p} \quad & \sum_{i\in S} E_p(U_i) \\
\text{s.t.} \quad & \sum_{\alpha_{-i}\in\Omega_{-i}} p(\alpha_i^*,\ \alpha_{-i})\left[U^{(i)}_{\alpha_i^*,\alpha_{-i}} - U^{(i)}_{\alpha_i,\alpha_{-i}}\right] \geqslant 0, \\
& \qquad \forall \alpha_i, \alpha_i^* \in \Omega_i,\ \ \forall i \in S \\
& \sum_{\substack{\alpha_i^*\in\Omega_i,\\ \alpha_{-i}\in\Omega_{-i}}} p(\alpha_i^*,\ \alpha_{-i}) = 1 \forall i\ 0 \leq p(\alpha_i^*,\ \alpha_{-i}) \leq 1,
\end{aligned} \tag{11}$$

where $E_p(\cdot)$ denotes the expectation over the set of all probabilities. We can limit ourselves into 2-users 2-BSs scenario with N strategies. In such a case, the LP problem can be presented as follows:

$$\max_{p_{i,j}} \sum_{k=1}^{N}\sum_{l=1}^{N}\left(U^{(1)}_{k,l} + U^{(2)}_{k,l}\right)p_{k,l}, \tag{12}$$

where $U^{(i)}_{k,l}$ is the utility for player i when the joint action pair is $\{\alpha_i^{(k)},\ \alpha_{-i}^{(l)}\}$ and $p_{k,l} = p(\alpha_i^{(k)},\ \alpha_{-i}^{(l)})$ is the corresponding joint probability for that action pair. The first correlated equilibrium constraint can be presented in matrix form with the following inequality:

$$\mathbf{A}\cdot\mathbf{P} \geqslant \mathbf{0}$$

$$\mathbf{A} = \begin{pmatrix}
U^{(1)}_{1,1}-U^{(1)}_{2,1} & U^{(1)}_{1,2}-U^{(1)}_{2,2} & \cdots & U^{(1)}_{1,N_s}-U^{(1)}_{2,N_s} & 0 & 0 & \cdots & 0 & 0 & \cdots \\
U^{(1)}_{1,1}-U^{(1)}_{3,1} & U^{(1)}_{1,2}-U^{(1)}_{3,2} & \cdots & U^{(1)}_{1,N_s}-U^{(1)}_{3,N_s} & 0 & 0 & \cdots & 0 & 0 & \cdots \\
\vdots & \vdots & & \vdots & 0 & 0 & \cdots & 0 & 0 & \cdots \\
U^{(1)}_{1,1}-U^{(1)}_{N_s,1} & U^{(1)}_{1,2}-U^{(1)}_{N_s,2} & \cdots & U^{(1)}_{1,N_s}-U^{(1)}_{N_s,N_s} & 0 & 0 & \cdots & 0 & 0 & \cdots \\
0 & 0 & \cdots & 0 & U^{(1)}_{2,1}-U^{(1)}_{1,1} & U^{(1)}_{2,2}-U^{(1)}_{1,2} & \cdots & U^{(1)}_{2,N_s}-U^{(1)}_{1,N_s} & 0 & \cdots \\
0 & 0 & \cdots & 0 & U^{(1)}_{2,1}-U^{(1)}_{3,1} & U^{(1)}_{2,2}-U^{(1)}_{3,2} & \cdots & U^{(1)}_{2,N_s}-U^{(1)}_{3,N_s} & 0 & \cdots \\
0 & 0 & \cdots & 0 & \vdots & \vdots & & \vdots & 0 & \cdots \\
0 & 0 & \cdots & 0 & U^{(1)}_{2,1}-U^{(1)}_{N_s,1} & U^{(1)}_{2,2}-U^{(1)}_{N_s,2} & \cdots & U^{(1)}_{2,N_s}-U^{(1)}_{N_s,N_s} & 0 & \cdots \\
\vdots & & & & \vdots & \vdots & & \vdots & & \\
U^{(2)}_{1,1}-U^{(2)}_{2,1} & 0 & \cdots & 0 & U^{(2)}_{1,2}-U^{(2)}_{2,2} & 0 & \cdots & U^{(2)}_{1,N_s}-U^{(2)}_{2,N_s} & 0 & \cdots \\
U^{(2)}_{1,1}-U^{(2)}_{3,1} & 0 & \cdots & 0 & U^{(2)}_{1,2}-U^{(2)}_{3,2} & 0 & \cdots & U^{(2)}_{1,N_s}-U^{(2)}_{3,N_s} & 0 & \cdots \\
\vdots & 0 & & 0 & \vdots & 0 & \cdots & \vdots & 0 & \cdots \\
U^{(2)}_{1,1}-U^{(2)}_{N_s,1} & 0 & \cdots & 0 & U^{(2)}_{1,2}-U^{(2)}_{N_s,2} & 0 & \cdots & U^{(2)}_{1,N_s}-U^{(2)}_{N_s,N_s} & 0 & \cdots \\
0 & U^{(2)}_{2,1}-U^{(2)}_{1,1} & 0 & \cdots & 0 & U^{(2)}_{2,2}-U^{(2)}_{1,2} & 0 & \cdots & U^{(2)}_{2,N_s}-U^{(2)}_{1,N_s} & \cdots \\
0 & U^{(2)}_{2,1}-U^{(2)}_{3,1} & 0 & \cdots & 0 & U^{(2)}_{2,2}-U^{(2)}_{3,2} & 0 & \cdots & U^{(2)}_{2,N_s}-U^{(2)}_{3,N_s} & \cdots \\
0 & \vdots & 0 & \cdots & 0 & \vdots & 0 & & \vdots & \cdots \\
0 & U^{(2)}_{2,1}-U^{(2)}_{N_s,1} & 0 & \cdots & 0 & U^{(2)}_{2,2}-U^{(2)}_{N_s,2} & 0 & \cdots & U^{(2)}_{2,N_s}-U^{(2)}_{N_s,N_s} & \cdots \\
\vdots & \vdots & & & & \vdots & & & \vdots &
\end{pmatrix}$$

$$\mathbf{P}^T = \begin{pmatrix} p_{1,1} & p_{1,2} & \cdots & p_{1,N_s} & p_{2,1} & p_{2,2} & \cdots & p_{2,N_s} & p_{3,1} & \cdots & p_{N_s-1,N_s} & p_{N_s,1} & \cdots & p_{N_s,N_s-1} & p_{N_s,N_s} \end{pmatrix}. \tag{13}$$

Then, the augmented form of a LP problem can be formulated as

$$\begin{pmatrix} 1 & 0 & -\mathbf{c}^T_{1\times N_s^2} & \mathbf{0}_{1\times 2N_s^2-2N_s} & \mathbf{0}_{1\times N_s^2} \\ 0 & 1 & -\mathbf{1}_{1\times N_s^2} & \mathbf{0}_{1\times 2N_s^2-2N_s} & \mathbf{0}_{1\times N_s^2} \\ \mathbf{0}_{2N_s^2-2N_s\times 1} & \mathbf{0}_{2N_s^2-2N_s\times 1} & \mathbf{A}_{2N_s^2-2N_s\times N_s^2} & \mathbf{I}_{2N_s^2-2N_s\times 2N_s^2-2N_s} & \mathbf{0}_{2N_s^2-2N_s\times N_s^2} \\ \mathbf{0}_{N_s^2\times 1} & \mathbf{1}_{N_s^2\times 1} & -\mathbf{I}_{N_s^2\times N_s^2} & \mathbf{0}_{N_s^2\times 2N_s^2-2N_s} & \mathbf{I}_{N_s^2\times N_s^2} \end{pmatrix} \begin{pmatrix} Z \\ 1 \\ \mathbf{P}_{N_s^2\times 1} \\ \mathbf{x}^{(s1)}_{2N_s^2-2N_s\times 1} \\ \mathbf{x}^{(s2)}_{N_s^2\times 1} \end{pmatrix} = (\mathbf{0}), \tag{14}$$

where $\mathbf{x}^{(s1)}$ and $\mathbf{x}^{(s2)}$ are vectors corresponding to the slack variables.

Let us denote a $N_s^2 - 1$ simplex of $\mathbf{R}^{N_s^2}$ as $\Delta^{N_s^2-1} = \{(p_{1,1}, \ldots, p_{N_s,N_s}) \in \mathbf{R}_+^{N_s^2} \mid p_{1,1} + \cdots + p_{N_s,N_s} = 1\}$. Assuming $N_c = N_t$ transmit-receive antennas or equivalently $N_c = N$ codewords in the codebook, the solution of the LP problem formulated above is one of the vertexes of the polyhedron (i.e., $((N_c+2)^n)$-hedron), where the number of vertexes is equal to $(N_c+2)^n - 1$ and each vertex is $\Delta^{N_s^2-1}$.

Several of the vertexes correspond to the Nash Equilibrium (NE), specifically the ones that are the solution if $U^{(1)}_{k,l} + U^{(2)}_{k,l}$, $l \neq k$ is the largest among all $U^{(1)}_{k,l} + U^{(2)}_{k,l}$. However, it may be more beneficial when all players cooperate; that is, for $U^{(1)}_{k,l} + U^{(2)}_{k,l}$, $l = k$, especially in case of severe interference between the players, thus the correlated equilibrium may be the optimal strategy.

A well-known Simplex algorithm [13] can be applied to solve the formulated problem, but the number of necessary operations is extremely high, especially when the number of available strategies increases. Moreover, extensive signaling might be necessary to provide all the required information to solve the presented problem. Thus, a distributed and iterative learning solution is more suitable to find the optimal time sharing coefficients.

4. Mechanism Design and Learning Algorithm

The rate optimization over the interference channel requires two major issues to be coped with: first, ensure the system convergence to the desired point, that can be achieved using an auction utility function; second, a distributed solution is necessary to achieve the equilibrium, such as the proposed regret-matching algorithm.

4.1. Mechanism Designed Utility. To resolve any conflicts between users, the Vickrey-Clarke-Groves (VCG) auction mechanism design is employed, which aims to maximize the utility U_i, for all i, defined as

$$U_i \triangleq R_i - \zeta_i, \tag{15}$$

where R_i is the rate of user i, and the cost ζ_i is evaluated as

$$\zeta_i(\alpha) = \sum_{j\neq i} R_j(\boldsymbol{\alpha}_{-i}) - \sum_{j\neq i} R_j(\alpha_i). \tag{16}$$

Hence, for the considered scenario with two users the payment costs for user 1 can be defined as

$$\begin{aligned} &\zeta_1\left(\alpha_1 \mathrel{\widehat{=}} \mathbf{Q}_1^{(k)},\ \alpha_2 \mathrel{\widehat{=}} \mathbf{Q}_2^{(l)}\right) \\ &\quad = R_2\left(\alpha_1 \mathrel{\widehat{=}} \mathbf{Q}_1^{(0)},\ \alpha_2 \mathrel{\widehat{=}} \mathbf{Q}_2^{(l)}\right) - R_2\left(\alpha_1 \mathrel{\widehat{=}} \mathbf{Q}_1^{(k)},\ \alpha_2 \mathrel{\widehat{=}} \mathbf{Q}_2^{(l)}\right) \\ &\quad = \log_2\left(\det\left(\mathbf{I} + \left(\mathbf{H}_{22}\mathbf{Q}_2^{(l)}\mathbf{H}_{22}^*\right)\cdot\sigma^{-2}\right)\right) \\ &\qquad - \log_2\left(\det\left(\mathbf{I} + \mathbf{H}_{22}\mathbf{Q}_2^{(l)}\mathbf{H}_{22}^* \cdot \left(\sigma^2\mathbf{I} + \mathbf{H}_{12}\mathbf{Q}_1^{(k)}\mathbf{H}_{12}\right)^{-1}\right)\right), \end{aligned} \tag{17}$$

where $\mathbf{Q}_1^{(k)}$ and $\mathbf{Q}_2^{(l)}$ are the covariance matrices corresponding to the strategies $\alpha_1^{(k)}$ and $\alpha_2^{(l)}$ selected by user 1 and user 2, respectively, what is denoted $\alpha_i \mathrel{\widehat{=}} \mathbf{Q}_i^{(k)}$. The payment cost ζ_2 follows by symmetry. Thus, the VCG utilities can be calculated using

$$\{U_1,\ U_2\} = \left\{U_1'\left(\mathbf{Q}_1^{(k)},\ \mathbf{Q}_2^{(l)}\right),\ U_2'\left(\mathbf{Q}_1^{(k)},\ \mathbf{Q}_2^{(l)}\right)\right\}, \tag{18}$$

where $U_1'(\mathbf{Q}_1^{(k)}, \mathbf{Q}_2^{(l)})$ and $U_2'(\mathbf{Q}_1^{(k)}, \mathbf{Q}_2^{(l)})$ for the considered cases are defined as in (19), (22), and (24), respectively.

4.2. The TSD-MIMO Case. In the investigated TSD-MIMO scenario, no transmit and receive beamforming is applied, and the considered strategies represent the transmit antenna selection mechanism. Hence, the VCG utilities can be calculated as in (19). The first part of both equations presents the achievable rate (payoff) of the ith user if no auction theory is applied (no cost is paid by the user for starting playing). On the other hand, last two parts express the price ζ_i (defined as 18) to be paid by the ith user for playing the chosen strategy

$$\begin{aligned} &U_1'\left(\mathbf{Q}_1^{(k)},\ \mathbf{Q}_2^{(l)}\right) \\ &= \log_2\left(\det\left(\mathbf{I} + \mathbf{H}_{11}\mathbf{Q}_1^{(k)}\mathbf{H}_{11}^* \cdot \left(\sigma^2\mathbf{I} + \mathbf{H}_{21}\mathbf{Q}_2^{(l)}\mathbf{H}_{21}\right)^{-1}\right)\right) \\ &\quad - \log_2\left(\det\left(\mathbf{I} + \mathbf{H}_{22}\mathbf{Q}_2^{(l)}\mathbf{H}_{22}^*\sigma^{-2}\right)\right) \\ &\quad + \log_2\left(\det\left(\mathbf{I} + \mathbf{H}_{22}\mathbf{Q}_2^{(l)}\mathbf{H}_{22}^* \cdot \left(\sigma^2\mathbf{I} + \mathbf{H}_{12}\mathbf{Q}_1^{(k)}\mathbf{H}_{12}\right)^{-1}\right)\right), \end{aligned}$$

$$
\begin{aligned}
&U_2'\left(\mathbf{Q}_1^{(k)},\ \mathbf{Q}_2^{(l)}\right)\\
&= \log_2\left(\det\left(\mathbf{I}+\mathbf{H}_{22}\mathbf{Q}_2^{(l)}\mathbf{H}_{22}^{*}\cdot\left(\sigma^2\mathbf{I}+\mathbf{H}_{12}\mathbf{Q}_1^{(k)}\mathbf{H}_{12}\right)^{-1}\right)\right)\\
&\quad-\log_2\left(\det\left(\mathbf{I}+\mathbf{H}_{11}\mathbf{Q}_1^{(k)}\mathbf{H}_{11}^{*}\sigma^{-2}\right)\right)\\
&\quad+\log_2\left(\det\left(\mathbf{I}+\mathbf{H}_{11}\mathbf{Q}_1^{(k)}\mathbf{H}_{11}^{*}\cdot\left(\sigma^2\mathbf{I}+\mathbf{H}_{21}\mathbf{Q}_2^{(l)}\mathbf{H}_{21}\right)^{-1}\right)\right).
\end{aligned}
\tag{19}
$$

Since the precoding vectors in case of TSD-MIMO correspond to the selection of one of the available transmit antennas (or the selection of both with equal power distribution), there are only four strategies are available to users, which correspond to the following covariance matrices:

$$
\begin{aligned}
&\mathbf{Q}_i^{(0)}=\begin{pmatrix}0&0\\0&0\end{pmatrix},\qquad \mathbf{Q}_i^{(1)}=\begin{pmatrix}P_{i,\max}&0\\0&0\end{pmatrix},\\
&\mathbf{Q}_i^{(2)}=\begin{pmatrix}0&0\\0&P_{i,\max}\end{pmatrix},\qquad \mathbf{Q}_i^{(3)}=\begin{pmatrix}\frac{P_{i,\max}}{2}&0\\0&\frac{P_{i,\max}}{2}\end{pmatrix}.
\end{aligned}
\tag{20}
$$

When selecting the strategy corresponding to $\mathbf{Q}_i^{(0)}$ user i decides to remain silent. On the contrary, $\mathbf{Q}_i^{(1)}$ and $\mathbf{Q}_i^{(2)}$ correspond to the situation when user i decides to transmit on antenna 1 or antenna 2, respectively. Finally, $\mathbf{Q}_i^{(3)}$ is the covariance matrix representing the strategy when user i transmits on both antennas with equal power distribution.

4.3. The OFDM Case. One may observe that the proposed general mechanism design can be used to investigate the performance of OFDM transmission on the interference channel. This is the case when the channel matrices $\mathbf{H}_{ij}$, for all $\{i,\ j\}$ are diagonal, so the specific paths represent the orthogonal subcarriers. Similarly to the previous subsection, first parts of the equations present the achievable rate (payoff) of the ith user if no auction theory is applied (no cost is paid by the user for starting playing). Next, last two parts defines the price ζ_i (defined as 18) to be paid by the ith user for starting playing the chosen strategy. It is worth mentioning that since the above-mentioned $\mathbf{H}$ matrix is diagonal one can easily apply the eigenvalue decomposition (or singular value decomposition) to reduce the number of required operations. Hence, for the considered 2-user scenario the cost for user i can be evaluated as in (21), and the VCG utilities can be defined as in (22). For the sake of clarity, let us provide the interpretation of selected variables in the equations below for the OFDM case: $h_{k,k}^{(i,j)}$ is the channel coefficient that characterizes the channel on the kth subcarriers between the ith and the jth user and $q_{k,k}^{(i)}$ is the kth diagonal element from the considered covariance matrix $\mathbf{Q}^{(i)}$ of the ith user

$$
\begin{aligned}
&\zeta_1\left(\alpha_1\mathrel{\widehat{=}}\mathbf{Q}_1^{(k)},\ \alpha_2\mathrel{\widehat{=}}\mathbf{Q}_2^{(l)}\right)\\
&\quad=R_2\left(\alpha_1\mathrel{\widehat{=}}\mathbf{Q}_1^{(0)},\ \alpha_2\mathrel{\widehat{=}}\mathbf{Q}_2^{(l)}\right)-R_2\left(\alpha_1\mathrel{\widehat{=}}\mathbf{Q}_1^{(k)},\ \alpha_2\mathrel{\widehat{=}}\mathbf{Q}_2^{(l)}\right)\\
&\quad=\log_2\left(1+\frac{q_{11}^{(2)}\left|h_{11}^{(22)}\right|^2}{\sigma_n^2}\right)+\log_2\left(1+\frac{q_{22}^{(2)}\left|h_{22}^{(22)}\right|^2}{\sigma_n^2}\right)\\
&\qquad-\log_2\left(1+\frac{q_{11}^{(2)}\left|h_{11}^{(22)}\right|^2}{\sigma_n^2+q_{11}^{(1)}\left|h_{11}^{(12)}\right|^2}\right)\\
&\qquad-\log_2\left(1+\frac{q_{22}^{(2)}\left|h_{22}^{(22)}\right|^2}{\sigma_n^2+q_{22}^{(1)}\left|h_{22}^{(12)}\right|^2}\right),\\
&\zeta_2\left(\alpha_1\mathrel{\widehat{=}}\mathbf{Q}_1^{(k)},\ \alpha_2\mathrel{\widehat{=}}\mathbf{Q}_2^{(l)}\right)\\
&\quad=R_1\left(\alpha_1\mathrel{\widehat{=}}\mathbf{Q}_1^{(k)},\ \alpha_2\mathrel{\widehat{=}}\mathbf{Q}_2^{(0)}\right)-R_1\left(\alpha_1\mathrel{\widehat{=}}\mathbf{Q}_1^{(k)},\ \alpha_2\mathrel{\widehat{=}}\mathbf{Q}_2^{(l)}\right)\\
&\quad=\log_2\left(1+\frac{q_{11}^{(1)}\left|h_{11}^{(11)}\right|^2}{\sigma_n^2}\right)+\log_2\left(1+\frac{q_{22}^{(1)}\left|h_{22}^{(11)}\right|^2}{\sigma_n^2}\right)\\
&\qquad-\log_2\left(1+\frac{q_{11}^{(1)}\left|h_{11}^{(11)}\right|^2}{\sigma_n^2+q_{11}^{(2)}\left|h_{11}^{(21)}\right|^2}\right)\\
&\qquad-\log_2\left(1+\frac{q_{22}^{(1)}\left|h_{22}^{(11)}\right|^2}{\sigma_n^2+q_{22}^{(2)}\left|h_{22}^{(21)}\right|^2}\right),
\end{aligned}
\tag{21}
$$

$$
\begin{aligned}
&U_1\left(\mathbf{Q}_1^{(k)},\ \mathbf{Q}_2^{(l)}\right)\\
&=\log_2\left(1+\frac{q_{11}^{(1)}\left|h_{11}^{(11)}\right|^2}{\sigma_n^2+q_{11}^{(2)}\left|h_{11}^{(21)}\right|^2}\right)\\
&\quad+\log_2\left(1+\frac{q_{22}^{(1)}\left|h_{22}^{(11)}\right|^2}{\sigma_n^2+q_{22}^{(2)}\left|h_{22}^{(21)}\right|^2}\right)-\zeta_1\left(\alpha_1\mathrel{\widehat{=}}\mathbf{Q}_1^{(k)},\ \alpha_2\mathrel{\widehat{=}}\mathbf{Q}_2^{(l)}\right),\\
&U_2\left(\mathbf{Q}_1^{(k)},\ \mathbf{Q}_2^{(l)}\right)\\
&=\log_2\left(1+\frac{q_{11}^{(2)}\left|h_{11}^{(22)}\right|^2}{\sigma_n^2+q_{11}^{(1)}\left|h_{11}^{(12)}\right|^2}\right)\\
&\quad+\log_2\left(1+\frac{q_{22}^{(2)}\left|h_{22}^{(22)}\right|^2}{\sigma_n^2+q_{22}^{(1)}\left|h_{22}^{(12)}\right|^2}\right)-\zeta_2\left(\alpha_1\mathrel{\widehat{=}}\mathbf{Q}_1^{(k)},\ \alpha_2\mathrel{\widehat{=}}\mathbf{Q}_2^{(l)}\right).
\end{aligned}
\tag{22}
$$

4.4. The Precoded MIMO Case. Obviously, the idea of correlated equilibrium and of application of the auction theorem, described in the previous subsections, can be applied also for the precoded MIMO case. However, beside the straightforward modification of the equations describing the payment cost (see (23)), and VCG utilities (see (24)) the set of possible strategies has to be interpreted in a different way. However, following the way provided in the previous subsections, one can interpret the equations presented below in more detailed way. Thus, the first part of (24) presents the achievable rate (payoff) of the ith user if no auction theory is applied (no cost is paid by the user for starting playing), whereas last two parts express the price ζ_i (defined as 18) to be paid by the ith user for starting playing the chosen strategy

$$\zeta_1\left(\alpha_1 \widehat{=} \mathbf{Q}_1^{(k)},\ \alpha_2 \widehat{=} \mathbf{Q}_2^{(l)}\right)$$
$$= R_2\left(\alpha_1 \widehat{=} \mathbf{Q}_1^{(0)},\ \alpha_2 \widehat{=} \mathbf{Q}_2^{(l)}\right) - R_2\left(\alpha_1 \widehat{=} \mathbf{Q}_1^{(k)},\ \alpha_2 \widehat{=} \mathbf{Q}_2^{(l)}\right)$$
$$= \log_2\left(\det\left(I + \mathbf{u}_2^* \mathbf{H}_{22}\mathbf{v}_2\mathbf{Q}_2^{(l)}\mathbf{v}_2^*\mathbf{H}_{22}^*\mathbf{u}_2 \cdot \sigma^{-2}\right)\right)$$
$$- \log_2\left(\det\left(I + \mathbf{u}_2^* \mathbf{H}_{22}\mathbf{v}_2\mathbf{Q}_2^{(l)}\mathbf{v}_2^*\mathbf{H}_{22}^*\mathbf{u}_2 \cdot \left(\sigma^2\mathbf{u}_2^*\mathbf{u}_2 + \mathbf{u}_2^*\mathbf{H}_{12}\mathbf{v}_1\mathbf{Q}_1^{(k)}\mathbf{v}_1^*\mathbf{H}_{12}\mathbf{u}_2\right)^{-1}\right)\right),$$

$$\zeta_2\left(\alpha_1 \widehat{=} \mathbf{Q}_1^{(k)},\ \alpha_2 \widehat{=} \mathbf{Q}_2^{(l)}\right)$$
$$= R_1\left(\alpha_1 \widehat{=} \mathbf{Q}_1^{(k)},\ \alpha_2 \widehat{=} \mathbf{Q}_2^{(0)}\right) - R_1\left(\alpha_1 \widehat{=} \mathbf{Q}_1^{(k)},\ \alpha_2 \widehat{=} \mathbf{Q}_2^{(l)}\right)$$
$$= \log_2\left(\det\left(I + \mathbf{u}_1^* \mathbf{H}_{11}\mathbf{v}_1\mathbf{Q}_1^{(k)}\mathbf{v}_1^*\mathbf{H}_{11}^*\mathbf{u}_1 \cdot \sigma^{-2}\right)\right)$$
$$- \log_2\left(\det\left(I + \mathbf{u}_1^* \mathbf{H}_{11}\mathbf{v}_1\mathbf{Q}_1^{(k)}\mathbf{v}_1^*\mathbf{H}_{11}^*\mathbf{u}_1 \cdot \left(\sigma^2\mathbf{u}_1^*\mathbf{u}_1 + \mathbf{u}_1^*\mathbf{H}_{21}\mathbf{v}_2\mathbf{Q}_2^{(l)}\mathbf{v}_2^*\mathbf{H}_{21}\mathbf{u}_1\right)^{-1}\right)\right),$$

$$U_1'\left(\mathbf{Q}_1^{(k)},\ \mathbf{Q}_2^{(l)}\right) \tag{23}$$
$$= \log_2\left(\det\left(\mathbf{I} + \mathbf{u}_1^* \mathbf{H}_{11}\mathbf{v}_1\mathbf{Q}_1^{(k)}\mathbf{v}_1^*\mathbf{H}_{11}^*\mathbf{u}_1 \cdot \left(\sigma^2\mathbf{u}_1^*\mathbf{u}_1 + \mathbf{u}_1^*\mathbf{H}_{21}\mathbf{v}_2\mathbf{Q}_2^{(l)}\mathbf{v}_2^*\mathbf{H}_{21}\mathbf{u}_1\right)^{-1}\right)\right)$$
$$- \log_2\left(\det\left(\mathbf{I} + \mathbf{u}_2^* \mathbf{H}_{22}\mathbf{v}_2\mathbf{Q}_2^{(l)}\mathbf{v}_2^*\mathbf{H}_{22}^*\mathbf{u}_2\sigma^{-2}\right)\right)$$
$$+ \log_2\left(\det\left(\mathbf{I} + \mathbf{u}_2^* \mathbf{H}_{22}\mathbf{v}_2\mathbf{Q}_2^{(l)}\mathbf{v}_2^*\mathbf{H}_{22}^*\mathbf{u}_2 \cdot \left(\sigma^2\mathbf{u}_2^*\mathbf{u}_2 + \mathbf{u}_2^*\mathbf{H}_{12}\mathbf{v}_1\mathbf{Q}_1^{(k)}\mathbf{v}_1^*\mathbf{H}_{12}\mathbf{u}_2\right)^{-1}\right)\right),$$

$$U_2'\left(\mathbf{Q}_1^{(k)},\ \mathbf{Q}_2^{(l)}\right)$$
$$= \log_2\left(\det\left(\mathbf{I} + \mathbf{u}_2^* \mathbf{H}_{22}\mathbf{v}_2\mathbf{Q}_2^{(l)}\mathbf{v}_2^*\mathbf{H}_{22}^*\mathbf{u}_2 \cdot \left(\sigma^2\mathbf{u}_2^*\mathbf{u}_2 + \mathbf{u}_2^*\mathbf{H}_{12}\mathbf{v}_1\mathbf{Q}_1^{(k)}\mathbf{v}_1^*\mathbf{H}_{12}\mathbf{u}_2\right)^{-1}\right)\right)$$
$$- \log_2\left(\det\left(\mathbf{I} + \mathbf{u}_1^* \mathbf{H}_{11}\mathbf{v}_1\mathbf{Q}_1^{(k)}\mathbf{v}_1^*\mathbf{H}_{11}^*\mathbf{u}_1\sigma^{-2}\right)\right)$$
$$+ \log_2\left(\det\left(\mathbf{I} + \mathbf{u}_1^* \mathbf{H}_{11}\mathbf{v}_1\mathbf{Q}_1^{(k)}\mathbf{v}_1^*\mathbf{H}_{11}^*\mathbf{u}_1 \cdot \left(\sigma^2\mathbf{u}_1^*\mathbf{u}_1 + \mathbf{u}_1^*\mathbf{H}_{21}\mathbf{v}_2\mathbf{Q}_2^{(l)}\mathbf{v}_2^*\mathbf{H}_{21}\mathbf{u}_1\right)^{-1}\right)\right). \tag{24}$$

In the previous cases (i.e., TSD-MIMO and OFDM), the selection of one of the predefined strategies means that the BS selects first, second, or both antennas for transmission or is silent. In the SVD-MIMO case, the selection of the covariance matrix Q_i by the BS has an interpretation of choosing one of the calculated singular values (obtained as the result of singular value decomposition of the transfer channel matrix). Thus, for example, by choosing the strategy corresponding to $\mathbf{Q}_i^1$ means that we choose the first singular value and—in consequence—the transmit and receive precoding vector that correspond to this singular value. Moreover, selection of the third strategy corresponding to $\mathbf{Q}_i^3$ has a meaning that no specific precoding has to be applied. Such, situation can occur in a presence of high interference between adjacent cells. It has to be stressed that selection of the first strategy will be preferred since the precoding vectors that correspond to this particular singular value maximize the channel capacity. However, this statement can be no longer valid in a strong interference case. The obtained results show that in such a situation, the proposed algorithm (that will be described later) converges to global optimum when the second or even third strategy is selected.

Different interpretation of the user strategies has to be defined for the ZF/MMSE/ML-MIMO transmission when the codebook of size N is used. In such a case, the number of strategies has to be increased from 4 (as in TSD-MIMO case) to $N + 2$, that is, the player (BS) can choose to be silent (one strategy), not to use any specific beamformer (second strategy), or to use one of the predefined and stored in a codebook strategies (remaining N strategies).

4.5. The Regret-Matching Algorithm. In [8], the regret-matching learning algorithm is proposed to learn in a distributive fashion how to achieve the correlated equilibrium set in solving the VCG auction. Since in [8] the interference channel with only one transmit and one receive antenna per user is considered, there are only two distinct binary actions $\alpha_i^{(0)} = 0$ and $\alpha_i^{(1)} = P_{\max}$ at every time $t = T$. However, in case of the considered MIMO interference channel with 2×2 configuration, there are more actions possible. Hence, the regret REG_i^T of user i at time T for playing action $\alpha_i^{(k)}$ instead of other actions is

$$\mathrm{REG}_i^T\left(\alpha_i^{(k)},\ \boldsymbol{\alpha}_{\mathbf{i}}^{(-\mathbf{k})}\right) \triangleq \max\left\{D_i^T\left(\alpha_i^{(k)},\ \boldsymbol{\alpha}_{\mathbf{i}}^{(-\mathbf{k})}\right),\ 0\right\}, \tag{25}$$

where

$$D_i^T\left(\alpha_i^{(k)},\ \boldsymbol{\alpha}_{\mathbf{i}}^{(-\mathbf{k})}\right) = \frac{1}{T}\sum_{\substack{j=1 \\ j \neq k}}^{K}\sum_{t \leq T}\left(U_i^t\left(\alpha_i^{(j)},\ \boldsymbol{\alpha}_{-\mathbf{i}}\right) - U_i^t\left(\alpha_i^{(k)},\ \boldsymbol{\alpha}_{-\mathbf{i}}\right)\right), \tag{26}$$

where K is the cardinality of the set of all actions available to user i, $U_i^t(\alpha_i^{(\cdot)}, \boldsymbol{\alpha}_{-\mathbf{i}})$ is the utility at time t, and $\boldsymbol{\alpha}_{-\mathbf{i}}$ is the vector specifying the other users actions. $D_i^T(\alpha_i^{(k)}, \boldsymbol{\alpha}_{\mathbf{i}}^{(-\mathbf{k})})$ is the average payoff that user i would have obtained if it had played other action than $\alpha_i^{(k)}$ every time in the past. Other definitions of average payoff are possible, for example, finding the maximum value of average payoffs of all strategies other than k. The details of the regret-matching learning algorithm are presented in Algorithm 1. According to the theorem presented in [14], if every user plays according to the proposed learning algorithm, then the found probability distribution should converge on the set of correlated equilibrium as $T \to \infty$.

Initialize arbitrarily probability for user i, p_i
For $t = 2, 3, 4, \ldots$
(1) Let $\alpha_{i,\,t-1}^{(k)}$ be the action last chosen by user i, and $\boldsymbol{\alpha}_{\mathbf{i},\,\mathbf{t-1}}^{(-\mathbf{k})}$ as the other actions
(2) Find the $D_i^{t-1}(\alpha_{i,\,t-1}^{(k)},\ \boldsymbol{\alpha}_{\mathbf{i},\,\mathbf{t-1}}^{(-\mathbf{k})})$ as in (26)
(3) Find the average regret for playing k instead of any other action $-k$ as in (25)
$\mathrm{REG}_i^{t-1}(\alpha_{i,\,t-1}^{(k)},\ \boldsymbol{\alpha}_{\mathbf{i},\,\mathbf{t-1}}^{(-\mathbf{k})})$
(4) Calculate the $\mu^{(t-1)}$ factor value as: $\mu^{(t-1)} = \sum_k \mathrm{REG}_i^{t-1}(\alpha_{i,\,t-1}^{(k)},\ \boldsymbol{\alpha}_{\mathbf{i},\,\mathbf{t-1}}^{(-\mathbf{k})})/(K-1)$
(5) Find the probability distribution of the actions for the next period, defined as:
If for all $_k\mathrm{REG}_i^{t-1}(\alpha_{i,\,t-1}^{(k)},\ \boldsymbol{\alpha}_{\mathbf{i},\,\mathbf{t-1}}^{(-\mathbf{k})}) > 0$,
$p_i^t(\boldsymbol{\alpha}_{\mathbf{i},\,\mathbf{t}}^{(-\mathbf{k})}) = (1/\mu^{(t-1)})\mathrm{REG}_i^{t-1}(\alpha_{i,\,t-1}^{(k)},\ \boldsymbol{\alpha}_{\mathbf{i},\,\mathbf{t-1}}^{(-\mathbf{k})})$,
$p_i^t(\alpha_{i,\,t}^{(k)}) = 1 - (1/\mu^{(t-1)})\mathrm{REG}_i^{t-1}(\alpha_{i,\,t-1}^{(k)},\ \boldsymbol{\alpha}_{\mathbf{i},\,\mathbf{t-1}}^{(-\mathbf{k})})$
else
Find k where $\mathrm{REG}_i^{t-1}(\alpha_{i,\,t-1}^{(k)},\ \boldsymbol{\alpha}_{\mathbf{i},\,\mathbf{t-1}}^{(-\mathbf{k})}) = 0$. Set: $p_i^t(\alpha_{i,\,t}^{(k)}) = 1 p_i^t(\boldsymbol{\alpha}_{\mathbf{i},\,\mathbf{t}}^{(-\mathbf{k})}) = 0$

Algorithm 1: Regret-matching learning algorithm.

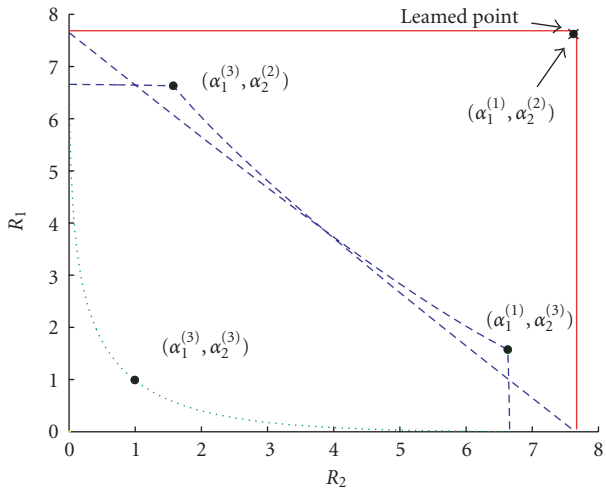

Figure 8: Crystallized rate regions in the interference limited case with marked learned point.

5. Simulation Results

5.1. Performance of the Regret-Matching Algorithm. To validate the correctness of the proposed idea, the 2-user 2×2 MIMO system has been simulated. In Figure 8, the crystallized rate region in the interference limited case has been shown, that is, the case when strong interference between antennas exist. The channel matrices for this case have been set as

$$\mathbf{H}_{11} = \begin{pmatrix} 1 & 1 \\ 0.01 & 0.01 \end{pmatrix}, \qquad \mathbf{H}_{22} = \begin{pmatrix} 0.01 & 0.01 \\ 1 & 1 \end{pmatrix},$$
$$\mathbf{H}_{12} = \begin{pmatrix} 0.01 & 0.01 \\ 1 & 1 \end{pmatrix}, \qquad \mathbf{H}_{21} = \begin{pmatrix} 1 & 1 \\ 0.01 & 0.01 \end{pmatrix}, \tag{27}$$

that implies that the first user observe strong interferences from the second user only on the second antenna while on the first antenna only the useful signal is received, and vice versa—the second users observes strong interference signal only on the first antenna. Such configuration explicitly leads toward choosing the strategy $\alpha^{(1)}$ and $\alpha^{(2)}$ by the first and second user, respectively, when the TSD-MIMO is considered. This is shown in Figure 8, where the solid line corresponds to the frontier lines. One can observe that indeed—the learned solution is that the regret matching algorithms converges to the point $(\alpha_1^{(1)},\ \alpha_2^{(2)})$. In other words, both users shall transmit with the maximum power all the times using the strategies $\alpha_1^{(1)}$ and $\alpha_2^{(2)}$, respectively.

In this figure, additional frontier lines of the possible rate regions when the users choose one (not optimal) of the possible strategies are presented; that is, the dotted line represents the frontier line when both users choose the strategy $\alpha_i^{(3)}$ all the time. This line corresponds to the interference limited SISO scenario in [8]. The dashed lines show the achievable rate regions boundaries, when one user plays the strategy $\alpha^{(3)}$ all the time, while the other transmit the whole power through one antenna.

In Figure 9, the achievable rate region for the noise limited scenario is presented, that is, both users observe the interferences coming from the neighboring cells, but the power of the interferences is significantly smaller than the power of the useful signal. In this figure, all 15 characteristic points have been presented, as well as the achievable rate region boundaries (dotted lines) when both players select one specific strategy and use them all the time. As expected, the learned point, that is, the point at the time-sharing line, that is, indicated by the regret-matching algorithm, corresponds to selecting the strategy $\alpha^{(3)}$ by both users all the time.

Moreover, in Figures 10 and 11 the convergence of the rate-matching algorithm in terms of number of iterations in the interference limited TSD-MIMO scenario has been presented. The same channel matrices have been used as in (27). One can notice that the algorithm have found the optimal solution extremely fast. Indeed, after around 10 iterations the learned point fits ideally to the optimum solution and remains unchanged.

Similar conclusions can be drawn for the precoded MIMO case. The rate region obtained for the SVD-MIMO

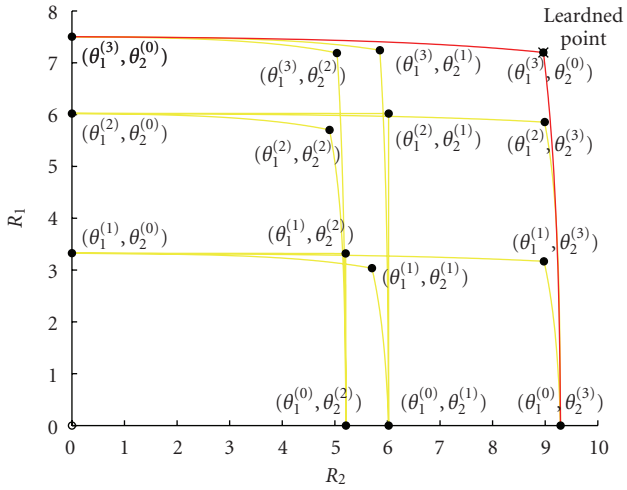

Figure 9: Crystallized rate regions in the noise-limited case with marked learned point.

case for a particular channel realization is presented in Figure 12. The interpretation of any point in the SVD rate region is as follows: both base stations use singular value decomposition in order to linearize the channel and the total transmit power is within the range $< 0,\ P_{\max} >$. Channel transfer matrices have been arbitrarily selected as follows:

$$\mathbf{H}_{11} = \begin{pmatrix} 0.9 & 0.00099 \\ 0.00085 & 0.96 \end{pmatrix},$$
$$\mathbf{H}_{22} = \begin{pmatrix} 0.96 & 0.000096 \\ 0.0000998 & 0.902 \end{pmatrix}$$
$$\mathbf{H}_{12} = \begin{pmatrix} 0.000094 & 0.00009 \\ 0.992 & 0.9992 \end{pmatrix}, \quad (28)$$
$$\mathbf{H}_{21} = \begin{pmatrix} 0.999 & 0.9904 \\ 0.0005 & 0.0001 \end{pmatrix},$$

that means that both users have good channel characteristic within their cells (no significant interference exist between the first transmit and second receive antenna as well as between second transmit and first receive antenna). However, first user causes strong interference on the second receive antenna of the second user, and the second users disturb significantly the signal received by the first user in his first antenna.

Analyzing the presented results one can observe that the obtained rate region is concave thus the time-sharing approach can provide better performance than continuous power control scheme (i.e., when both users transmit all the time and regulate the interference level by the means of the value of transmit power). The potential time-sharing Lines are presented in this figure. For the comparison purposes the line obtained for spatial waterfilling MIMO case has been plotted in Figure 12 (dotted line). The line has been derived in the following way: starting from point A (where user 2 does not transmit and user 1 uses the maximum power with the SWF technique) user 2 increases the total transmit power up to the maximum value, when both users transmit with the maximum total power point B is reached; finally user 1 decreases the transmit power from the maximum value to zero reaching the point C. Moreover, the power control line has been presented—it is the case when both users selects wrong strategy achieving extremely low rates. In is worth mentioning that the learned points obtained for various MIMO techniques have been marked in the described figure. One can observe that for the optimal case (SVD technique) algorithm converges to the point B. Slightly worse results have been obtained for TSD-MIMO, where no specific precoding has been performed. The worse results, but still in the vicinity of the point B, are for the random beamforming technique when 8 various precoders have been stored in a codebook and maximum likelihood method is used at the receiver.

Table 1: Achieved rates for channel definition (28).

MIMO scheme	User 1	User 2
TSD	13.17	12.77
SVD	13.17	13.28
ZF-RAN-8	5.12 (max. 12.24)	3.62 (max. 13.00)
MMSE-RAN-8	5.08 (max. 12.38)	3.64 (max. 13.13)
ML-RAN-8	12.51	11.81
ZF-LTE	12.87	12.98
MMSE-LTE	12.87	12.98
ML-LTE	12.90	13.00
ZF-PU^{2}RC-8	12.87	12.98
MMSE-PU^{2}RC-8	12.87	12.98
ML-PU^{2}RC-8	12.90	13.00

The same simulation have been carried out for other channel, when significant interference exist between all transmit and all receive antennas between ith user and ith BS. The channel transfer matrices have been selected as below:

$$\mathbf{H}_{11} = \begin{pmatrix} 0.4 & 0.49 \\ 0.52 & 0.46 \end{pmatrix}, \qquad \mathbf{H}_{22} = \begin{pmatrix} 0.45 & 0.49 \\ 0.47 & 0.45 \end{pmatrix},$$
$$\mathbf{H}_{12} = \begin{pmatrix} 0.000094 & 0.00009 \\ 0.992 & 0.9992 \end{pmatrix}, \qquad \mathbf{H}_{21} = \begin{pmatrix} 0.999 & 0.9904 \\ 0.0005 & 0.0001 \end{pmatrix}. \quad (29)$$

The obtained rate region, potential time-sharing lines, spatial waterfilling line and exemplary power control line, as well as some learned points (for the same MIMO techniques as described in the previous case) have been presented in Figure 13. One can observe that in such a case one of the learned points is close to the optimal one (Point B). However, this point is reached for random beamforming technique with maximum-likelihood method used at the receiver.

Specific rate values obtained for the considered MIMO implementations are given in Tables 1 and 2 for channel definitions (28) and (29), respectively. The results obtained for all RAN-8 scenarios (i.e., ZF, MMSE, and ML and

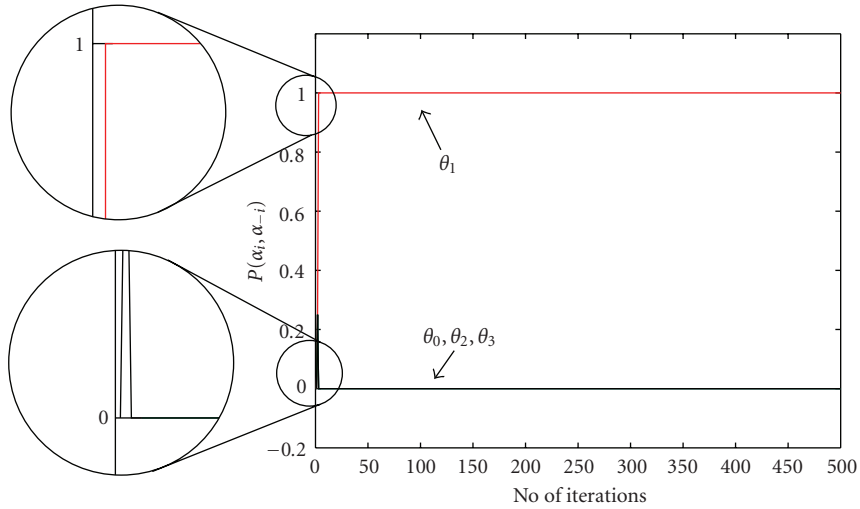

Figure 10: The convergence of the rate-matching algorithms—user 1.

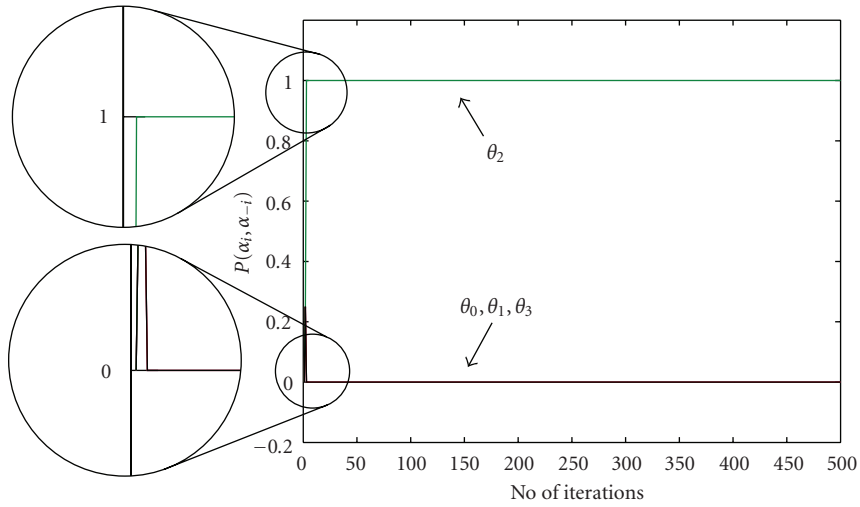

Figure 11: The convergence of the rate-matching algorithms—user 2.

Table 2: Achieved rates for channel definition (29).

MIMO scheme	User 1	User 2
TSD	11.40	11.23
SVD	12.23	12.11
ZF-RAN-8	4.25 (max. 11.25)	4.08 (max. 10.25)
MMSE-RAN-8	3.25 (max. 10.9)	4.07 (max. 11.05)
ML-RAN-8	12.08	11.95
ZF-LTE	12.13	11.96
MMSE-LTE	12.13	11.96
ML-LTE	12.89	12.93
ZF-PU^{2}RC-8	12.13	11.96
MMSE-PU^{2}RC-8	12.13	11.96
ML-PU^{2}RC-8	12.89	12.93

when the codebook size is equal to 8) have been averaged over 1000 randomly generated codebooks. One can observe that for all cases, when the regret-matching algorithm has been applied, the obtained rates are similar to each others and relatively close to the optimal solution. Only for the ZF/MMSE-MIMO cases when the random beamforming approach has been used, the averaged results are significantly worse because of high dependency of algorithms efficiency on the actual set of transmit beamformers. If the randomly generated set of beamformers is well defined (i.e., at least one precoder matches the actual channel conditions for ith user); the achieved rate is also close to the optimal point (see the maximum obtained values for one particular channel realization).

The efficiency of the random beamforming technique strongly depends on the number of precoders. However, the higher number of precoders the higher the complexity of the algorithm. Thus, in order to present the relation between the random beamforming technique efficiency and the codebook size the computer simulation have been carried

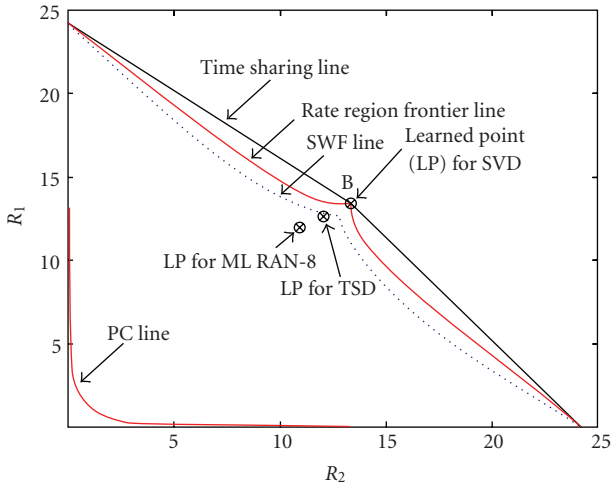

Figure 12: SVD-MIMO rate region—channel case 1.

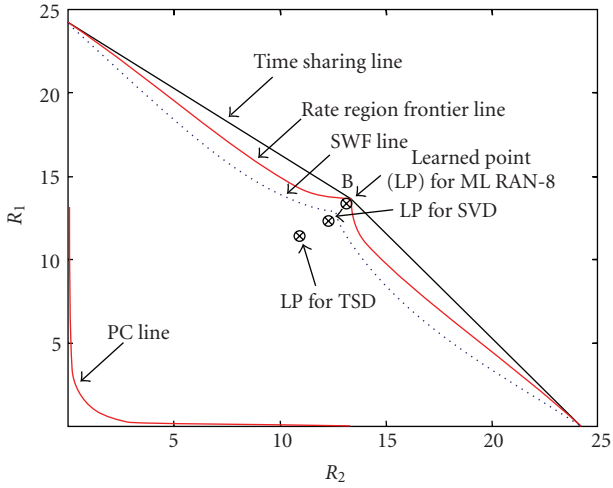

Figure 13: SVD-MIMO rate region—channel case 2.

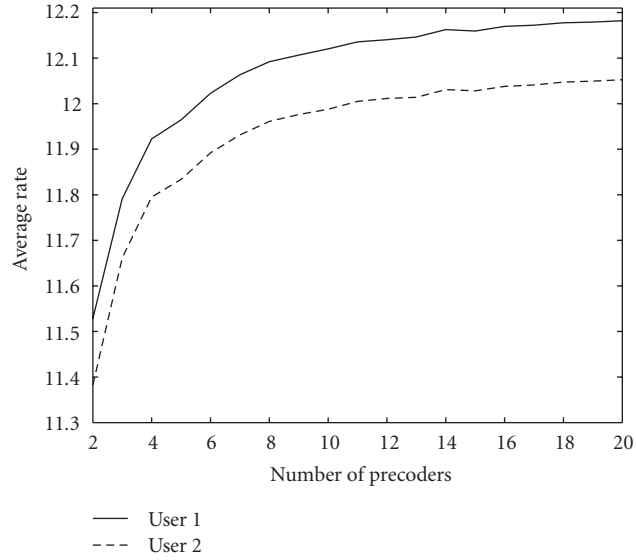

Figure 14: Achieved average rate versus codebook size.

out for the particular channel realization defined as above. The results, presented in Figure 14, have been obtained for 1000 various codebook realizations for each codebook size. One can observe that the obtained rate for both users increase logarithmically as the number of precoders increases.

5.2. The Regret-Matching Algorithm versus the Linear Programming Solution. In order to assess the efficiency of the proposed solution, the achievable sum rates versus the number of antennas have been compared for two cases: when the results have been obtained by application of the proposed regret-matching algorithm and by solving the linear programming problem defined in Section 3.1 . Two simulation scenarios have been selected for the 2-user 2-BSs MIMO configuration: TSD-MIMO and SVD-MIMO. The spatial waterfilling MIMO approach has been also considered for the comparison purposes. The Simplex algorithm [13] has been applied to solve the linear programming problem. The results obtained for the strong interference channel (similar to the one defined for 2×2 MIMO in (27)) are presented in Figure 15. One can observe that in both cases (linear programming and regret matching) the achieved sum rates are identical for both strategies when the number of antennas is higher than 2. Only for 2×2 MIMO case the proposed distributed solution performs slightly worse in terms of the achieved sum rate. It is particularly worth mentioning that the global optimum is reached in both cases. Similar results have been obtained also for the spatial waterfilling case. Let us stress that the complexity of the Simplex method is known to be polynomial whereas the complexity of the proposed regret-matching algorithm is linear [28]. In other words, the optimal solution is found at lower computation cost.

6. Conclusions

In this paper, the concept of crystallized rate regions, introduced first in the context of finding the capacity of the SISO interference channel, has been applied to the MIMO and OFDM interference channels. The idea of usage of the correlated equilibrium instead of the well-known Nash equilibrium has been verified adequate for the case of 2-user MIMO/OFDM transmission. A VCG auction utility function and the regret-matching algorithm have been derived for the generalized MIMO case. Simulation results for the selected 2-user scenarios proved the correctness of application of the crystallized rates region to the general MIMO and OFDM scenario. Moreover, obtained results show that the optimal solution is found—the strategies selected in the distributed case (by application of the regret-matching learning algorithm) are the same as the ones indicated by solving the linear programming problem.

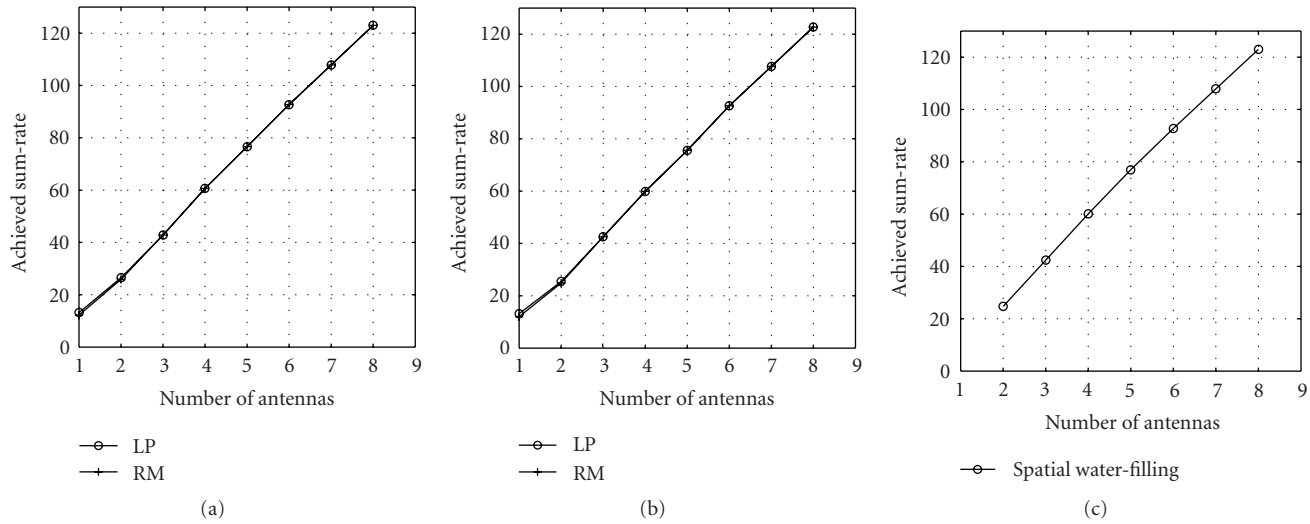

Figure 15: Achieved sum-rate versus the number of antennas for selected scenarios: (a) TSD-MIMO, (b) SVD-MIMO, and (c) spatial waterfilling reference line (LP: Linear Programming, RM: Regret Matching).

Acknowledgment

This paper was supported by the European Commission in the framework of the FP7 Network of Excellence in Wireless COMmunications NEWCOM++ (Contract no. 216715).

References

[1] E. Telatar, "Capacity of multi-antenna Gaussian channels," *European Transactions on Telecommunications*, vol. 10, no. 6, pp. 585–595, 1999.

[2] R. S. Blum, "MIMO capacity with interference," *IEEE Journal on Selected Areas in Communications*, vol. 21, no. 5, pp. 793–801, 2003.

[3] A. Sezgin, S. A. Jafar, and H. Jafarkhani, "Optimal use of antennas in interference networks: a tradeoff between rate, diversity and interference alignment," in *Proceedings of the IEEE Global Telecommunications Conference (GLOBECOM '09)*, Honolulu, Hawaii, USA, 2009.

[4] S. Annapureddy and V. V. Veeravalli, "Sum capacity of the Gaussian interference channel in the low interference regime," in *Proceedings of the Information Theory and Applications Workshop (ITA '08)*, pp. 422–427, San Diego, Calif, USA, February 2008.

[5] X. Shang, G. Kramer, and B. Chen, "Outer bound and noisy-interference sum-rate capacity for symmetric Gaussian interference channels," in *Proceedings of the 42nd Annual Conference on Information Sciences and Systems (CISS '08)*, pp. 385–389, Princeton, NJ, USA, March 2008.

[6] A. S. Motahari and A. K. Khandani, "Capacity bounds for the Gaussian interference channel," *IEEE Transactions on Information Theory*, vol. 55, no. 2, pp. 620–643, 2009.

[7] M. Charafeddine, A. Sezgin, and A. Paulraj, "Rates region frontiers for n-user interference channel with interference as noise," in *Proceedings of the Annual Allertone Conference on Communications, Control and Computing*, Allerton, Ill, USA, September 2007.

[8] M. Charafeddine, Z. Han, A. Paulraj, and J. Cioffi, "Crystallized rates region of the interference channel via correlated equilibrium with interference as noise," in *Proceedings of the IEEE International Conference on Communications (ICC '09)*, Dresden, Germany, June 2009.

[9] R. Ahlswede, "The capacity region of a channel with two senders and two receivers," *Annals of Probability*, vol. 2, no. 1, pp. 805–814, 1974.

[10] T. S. Han and K. Kobayashi, "A new achievable rates region for the interference channel," *IEEE Transactions on Information Theory*, vol. 27, no. 1, pp. 49–60, 1981.

[11] G. Owen, *Game Theory*, Academic, New York, NY, USA, 3rd edition, 2001.

[12] R. J. Aumann, "Subjectivity and correlation in randomized strategies," *Journal of Mathematical Economics*, vol. 1, no. 1, pp. 67–96, 1974.

[13] D. P. Bertsekas, A. Nedić, and A. E. Ozdaglar, *Convex Analysis and Optimization*, Athena Scientific, Belmont, Mass, USA, 2003.

[14] S. Hart and A. Mas-Colell, "A simple adaptive procedure leading to correlated equilibrium," *Econometrica*, vol. 68, no. 5, pp. 1127–1150, 2000.

[15] A. Kliks, P. Sroka, and M. Debbah, "MIMO crystallized rate regions," in *Proceedings of the European Wireless Conference (EW '10)*, pp. 940–947, Lucca, Italy, April 2010.

[16] A. Paulraj, R. Nabar, and D. Gore, *Introduction to Space-Time Wireless Communications*, Cambridge University Press, Cambridge, UK, 2003.

[17] G. Lebrun, J. Gao, and M. Faulkner, "MIMO transmission over a time-varying channel using SVD," *IEEE Transactions on Wireless Communications*, vol. 4, no. 2, pp. 757–764, 2005.

[18] K. Huang, J. G. Andrews, and R. W. Heath Jr., "Performance of orthogonal beamforming for SDMA with limited feedback," *IEEE Transactions on Vehicular Technology*, vol. 58, no. 1, pp. 152–164, 2009.

[19] D. Piazza and U. Spagnolini, "Random beamforming for spatial multiplexing in downlink multiuser MIMO systems," in *Proceedings of the IEEE International Symposium on Personal, Indoor and Mobile Radio Communications (PIMRC '05)*, vol. 4, pp. 2161–2165, Berlin, Germany, September 2005.

[20] 3GPP TS 36.211, "3rd Generation Partnership Project; Technical Specification Group Radio Access Network; Evolved Universal Terrestrial Radio Access (E-UTRA); Physical Channels andModulation (Release 8)," v. 8.4.0, September 2008.

[21] Samsung Electronics, "Downlink MIMO for EUTRA," 3GPP TSG RAN WG1 Meeting #44/R1-060335, February 2006.

[22] A. Goldsmith, S. A. Jafar, N. Jindal, and S. Vishwanath, "Fundamental capacity of MIMO channels," *IEEE Journal on Selected Areas in Communications*, vol. 21, 2002, *Special Issue on MIMO systems*.

[23] H. Dai, A. F. Molisch, and H. V. Poor, "Downlink capacity of interference-limited MIMO systems with joint detection," *IEEE Transactions on Wireless Communications*, vol. 3, no. 2, pp. 442–453, 2004.

[24] J. Choi, S. R. Kim, and I.-K. Choi, "Eigenbeamforming with selection diversity for MIMO-OFDM downlink," in *Proceedings of the IEEE 60th Vehicular Technology Conference (VTC '04)*, vol. 3, pp. 1806–1810, Los Angeles, Calif, USA, September 2004.

[25] M. Sharif and B. Hassibi, "On the capacity of MIMO broadcast channels with partial side information," *IEEE Transactions on Information Theory*, vol. 51, no. 2, pp. 506–522, 2005.

[26] Z. Shen, R. W. Heath Jr., J. G. Andrews, and B. L. Evans, "Space-time water-filling for composite MIMO fading channels," *Eurasip Journal on Wireless Communications and Networking*, vol. 2006, Article ID 16281, 8 pages, 2006.

[27] E. G. Larsson, E. A. Jorswieck, J. Lindblom, and R. Mochaourab, "Game theory and the flat-fading gaussian interference channel," *IEEE Signal Processing Magazine*, vol. 26, no. 5, pp. 18–27, 2009.

[28] B. Wang, Z. Han, and K. J. R. Liu, "Peer-to-peer file sharing game using correlated equilibrium," in *Proceedings of the 43rd Annual Conference on Information Sciences and Systems (CISS '09)*, pp. 729–734, March 2009.

[29] A. Calvó-armengol, "The Set of Correlated Equilibria of 2×2 Games," 2006, http://citeseerx.ist.psu.edu/viewdoc/summary?doi=10.1.1.119.8023.

Preliminary call for papers

The 2011 European Signal Processing Conference (EUSIPCO-2011) is the nineteenth in a series of conferences promoted by the European Association for Signal Processing (EURASIP, www.eurasip.org). This year edition will take place in Barcelona, capital city of Catalonia (Spain), and will be jointly organized by the Centre Tecnològic de Telecomunicacions de Catalunya (CTTC) and the Universitat Politècnica de Catalunya (UPC).

EUSIPCO-2011 will focus on key aspects of signal processing theory and applications as listed below. Acceptance of submissions will be based on quality, relevance and originality. Accepted papers will be published in the EUSIPCO proceedings and presented during the conference. Paper submissions, proposals for tutorials and proposals for special sessions are invited in, but not limited to, the following areas of interest.

Areas of Interest

- Audio and electro-acoustics.
- Design, implementation, and applications of signal processing systems.
- Multimedia signal processing and coding.
- Image and multidimensional signal processing.
- Signal detection and estimation.
- Sensor array and multi-channel signal processing.
- Sensor fusion in networked systems.
- Signal processing for communications.
- Medical imaging and image analysis.
- Non-stationary, non-linear and non-Gaussian signal processing.

Submissions

Procedures to submit a paper and proposals for special sessions and tutorials will be detailed at www.eusipco2011.org. Submitted papers must be camera-ready, no more than 5 pages long, and conforming to the standard specified on the EUSIPCO 2011 web site. First authors who are registered students can participate in the best student paper competition.

Important Deadlines:

Proposals for special sessions	15 Dec 2010
Proposals for tutorials	18 Feb 2011
Electronic submission of full papers	**21 Feb 2011**
Notification of acceptance	23 May 2011
Submission of camera-ready papers	6 Jun 2011

Webpage: www.eusipco2011.org

Organizing Committee

Honorary Chair
Miguel A. Lagunas (CTTC)

General Chair
Ana I. Pérez-Neira (UPC)

General Vice-Chair
Carles Antón-Haro (CTTC)

Technical Program Chair
Xavier Mestre (CTTC)

Technical Program Co-Chairs
Javier Hernando (UPC)
Montserrat Pardàs (UPC)

Plenary Talks
Ferran Marqués (UPC)
Yonina Eldar (Technion)

Special Sessions
Ignacio Santamaría (Unversidad de Cantabria)
Mats Bengtsson (KTH)

Finances
Montserrat Nájar (UPC)

Tutorials
Daniel P. Palomar (Hong Kong UST)
Beatrice Pesquet-Popescu (ENST)

Publicity
Stephan Pfletschinger (CTTC)
Mònica Navarro (CTTC)

Publications
Antonio Pascual (UPC)
Carles Fernández (CTTC)

Industrial Liaison & Exhibits
Angeliki Alexiou (University of Piraeus)
Albert Sitjà (CTTC)

International Liaison
Ju Liu (Shandong University-China)
Jinhong Yuan (UNSW-Australia)
Tamas Sziranyi (SZTAKI -Hungary)
Rich Stern (CMU-USA)
Ricardo L. de Queiroz (UNB-Brazil)